ISSN 1173-5996

Development of Bench-Scale Testing of Sprinkler and Smoke Detector Activation/Response Time

by

Kok Siong Chin

Supervised by:

Michael J Spearpoint

Fire Engineering Research Report 02/3

May 2002

This report was presented as a project report as part of the ME (Fire) Degree at the University of Canterbury

School of Engineering
University of Canterbury
Private Bag 4800
Christchurch, New Zealand

Phone 643 364-2250
Fax 643 364-2758
www.civil.canterbury.ac.nz

Abstract

In the past, many tests have been conducted to investigate the response of fire protection features such as sprinkler and smoke detector. Specifically designed apparatus have been designed for conducting such tests. For instance the plunge test apparatus and the FE/DE apparatus.

The intent of this research is to construct a bench-scale wind tunnel, which integrates the common features between the plunge test apparatus and FE/DE apparatus so that sprinkler and smoke detector can be tested using the same apparatus.

The scope of this report covers the design of the wind tunnel, and the selection of the individual component (test section, heating element, corners, dampers etc.). Several issues concerning the design and selection of the individual component are identified and discussed. These include the difficulties in finding a fan which would meet the design requirements (airflow velocity up to 2.5 m/s at a maximum of 300 °C operating temperature) at the test section, as well as the trade-off between selecting a high temperature rated fan and a high power rated heating element. Owing to a lack of time, the performance of the wind tunnel is not assessed. However, recommendations are given as how the wind tunnel's performance should be assessed in meeting the design requirements.

Acknowledgements

I would like to show my appreciation to the following people for their contributions towards the completion of this report.

1. *Mike Spearpoint,* who supervised and guided the development of this research,
2. *Nigel Dixon*, who helped in the co-ordination and construction of the wind tunnel,
3. *Grant Dunlop*, who helped in the co-ordination and construction of the wind tunnel,
4. *Alastair Young*, who helped in the design and construction of the wind tunnel.
5. *New Zealand Fire Service*, who help funded the Fire Engineering degree at the University of Canterbury.

Table of Contents

List of figures

List of tables

1. Literature research

Rapidly changing building designs, uses, materials, contents, fire protection and the general intermix of industrial/commercial and residential occupancies has created a need to understand the potential hazards and losses from fires and the performance of fire protection systems under conditions that may or may not be specifically addressed by historic fire testing and codes.

Fire protection strategies are designed and installed to perform specific functions. For instance, a fire sprinkler system is expected to control or extinguish fires. Likewise, a fire detection system is intended to provide sufficient early warning of a fire for occupant notification and escape, fire service notification and in some cases activation of other fire protection features (e.g. special extinguishing systems, smoke management systems). Both system activation (detection) and notification (alarm) must occur to achieve early warning. As such, the reliability of individual fire protection strategies such as detection and automatic suppression is an important input to detailed engineering analysis associated with performance-based design [24].

In the context of fire safety, there are several elements of reliability, including both the *operational reliability* and the *performance reliability*. The former provides a measure of probability that the fire protection system will operate as intended in fires (system operability) while the latter provides a measure of adequacy of the feature to successfully perform its intended function under specified fire condition (system adequacy).

Several studies have been reported by various organizations in estimating the reliability of fire protection systems. Table 1 provides the summary of such reports. Note that significant differences exist in the individual reliability estimates depending on the parameters used to develop these estimates. In addition, the uncertainty associated with a single estimate of reliability or the existence of potentially important biases in the methods used to derive these estimates may limit their direct usefulness in addressing either operational or performance reliability of fire protection systems.

Table 1: Published estimate of fire protection system operational reliability

(Probability of success (%))

Protection System	Warrington Delphi UK (Delphi Group)		Fire Eng Guidelines Australia (Expert Survey)		Japanese Studies (Incident Data)	
	Smoldering	Flaming	Smoldering	Flaming/ Flash Over	Tokyo FD	Watanabe
heat detector	0	89	0	90 / 95	94	89
home smoke alarm	76	79	65	75 / 74	NA	NA
system smoke detector	86	90	70	80 / 85	94	89
beam smoke detectors	86	88	70	80 / 85	94	89
aspirated smoke det.	86	NA	90	95 / 95	NA	NA
sprinklers operate	95		50	95 / 99	97	NA
sprinklers control but do not extinguish	64		NA		NA	NA
sprinklers extinguish	48		NA		96	NA
masonry construction	81 29% probability an opening will be fixed open		95 if no opening 90 if opening with auto closer		NA	NA
gypsum partitions	69 29% probability an opening will be fixed open		95 if no opening 90 if opening with auto closer		NA	NA

NA= Not Addressed

(Adopted from ref [24])

Table 2 provides a summary of reported operational reliability estimates from several studies that evaluated actual fire incidents in which automatic sprinklers were present. Although these estimates suggested a relatively high operational reliability for automatic sprinklers, the accuracy of such estimates must be accessed, primarily on the biases of the data sources and the uncertainties associated with combining data from different databases. Furthermore, factors such as the reporting time periods, the types of occupancies, and the level of detail regarding the types of fires and the sprinkler system design should also be considered. For instance, the high end estimates of 99.5 % reported by Maybee and Marryat reflected the sprinkler system performance in occupancies where inspection, testing and maintenance activities were rigorous and well documented.

Table 3 shows a summary of operational reliability estimates of fire detection/alarm system for selected occupancy groups, based on data provided by Hall [1995]. Note that the mean reliability estimates range from approximately 68 % to 88 %. The general range associated with the 95 % confidence interval is 66 % to 90 %.

Table 2: Reported automatic sprinkler reliability data (%)

Occupancy	Reference	Reliability Value
Commercial	Milne [1959]	96.6/97.6/89.2
	Automatic Sprinkler [1970]	90.8-98.2
	Miller [1974]	86
	DOE [1982]	98.9
	Maybee [1988]	99.5
	Kook [1990]	87.6
	Taylor [1990]	81.3
	Sprinkler Focus [1993]	98.4-95.8
	Linder [1993]	96
General	Building Research Est. [1973]	92.1
	Miller [1974]	95.8
	Miller [1974]	94.8
	Powers [1979]	96.2
	Richardson [1985]	96
	Finucane et al. [1987]	96.9-97.9
	Marryat [1988]	99.5
Residential	Milne [1959]	96.6
Institutional	Milne [1959]	96.6

Adopted from ref [24]

Table 3: Reliability estimates for smoke detectors

Occupancy	Property Use	Mean Reliability (%) n = 10	95% Upper Confidence Interval	95% Lower Confidence Interval
Residential	Apartments	69.3	69.9	68.7
	Hotels/Motels	77.8	79.3	76.4
	Dormitories	86.3	88.4	84.3
Commercial	Public Assembly	67.9	69.8	65.9
	Stores & Offices	71.7	73.5	69.9
	Storage	68.2	70.0	66.3
	Industry & Manufacturing	80.2	81.3	79.1
Institutional	Care of Aged	84.9	86.6	83.3
	Care of Young	84.0	86.3	81.6
	Educational	76.9	79.6	74.1
	Hospitals & Clinics	83.3	85.4	81.2
	Prisons & Jails	84.2	85.9	82.5
	Care of Mentally Handicapped	87.5	90.3	84.8

Adopted from ref [24]

Given the variations in the reliability estimates, and the uncertainties associated with these estimates, it is difficult for one to adopt a single value for any fire protection system design. Nevertheless, there is no doubt that when a fire protection system does operate, lives could be saved, and in some instances property damages could be minimised.

This is where the performance reliability comes in, where it is important that the fire protection features (sprinklers, smoke detectors etc.) performances be tested thoroughly before they are specified in any fire protection system design.

1.1 Sprinklers

Computer models have become the primary tools in enabling fire protection engineers to analyse fire protection problems. Thermal or sprinkler activation models are being used by fire protection engineers in the design and evaluation of fire suppression systems. Therefore it is important to know the accuracy and the limitations of the current sprinkler activation models.

Several studies have been conducted at the Building and Fire Research Laboratory of the National Institutes of Standards and Technology under the sponsorship of the General Services Administration to compare the experimental sprinkler activation time with the predictions from the computer models.

The large-scale compartment fire tests [25] were conducted in a space 18.9 m x 9.1 m with a ceiling height of 2.35 m. Four different types of sprinklers were studied; a quick-response bulb, a quick-response link, a standard-response bulb and a standard-response link. The ceiling of the compartment was composed of 12 mm thick gypsum board. The area of ceiling above the fire and continuing past the sprinkler measurement locations was covered with 12 mm thick calcium silicate board in addition to the gypsum board. The walls of the compartment were composed of concrete block.

The fire source for all the tests was a gaseous propane diffusion flame, with heat release rates (of steady-state fires) of 115 kW, 155 kW, 215 kW, and 290 kW at a

radial distance to ceiling height above the fuel (r/H) ratio of 0.67 and 290 kW and 520 kW at an r/H ratio of 1.3. Three replicates tests were conducted for each scenario.

After comparing the measured sprinkler activation times of the large-scale compartment tests with the predicted activation times from the models, the studies concluded that none of the computer models provided an accurate prediction for all the cases.

Clearly, much work is yet to be done in order to characterize the thermal response characteristics of sprinklers (activation time and RTI). Thus it is the intention of this research to develop a wind tunnel for conducting bench-scale testing of sprinklers to look into the characterization issues. Generally, there are two types of tests for sprinklers; I) Rate of rise test, and II) Plunge test [13].

1.1.1 Rate of rise test

The rate of rise test is used to determine the sensitivity characteristic of sprinklers to determine their suitability for use in applications specifying particular performance criteria. Generally, tests are undertaken at the following rates of temperature rise;

1. 2 °C/min
2. 12 °C/min
3. 20 °C/min

The sprinkler operating time is measured from initiation of the rate of rise, starting at a stable condition of 30 °C.

1.1.2 Plunge test

The plunge test apparatus (Fig. 1.1) was first developed for use with sprinklers in 1976. It consists of a wind tunnel, with a recirculating air at known temperature and velocity. The air temperature is set well above the nominal operating temperature of the sprinklers ($T_A > T_{ACT}$). At time t = 0, a sprinkler head is inserted (i.e., "plunged") into the heated air. The amount of time it takes for the sprinkler to operate is recorded

and is presumed to be the time it takes for the sprinkler operating mechanism to move from ambient temperature to the nominal operating temperature.

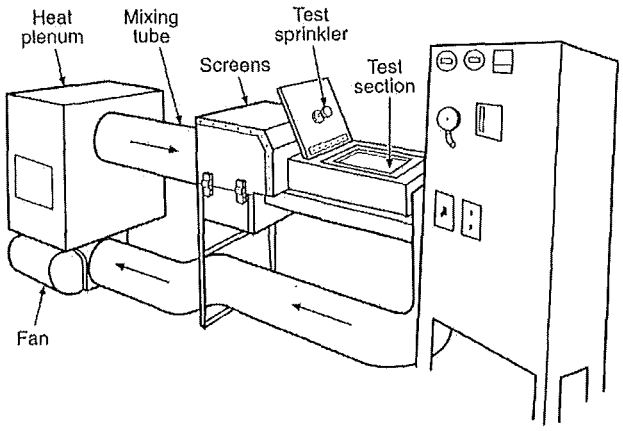

(Adopted from ref [9])

Figure 1.1 Sprinkler plunge test apparatus

The plunge test is used for two reasons;

1. It efficiently determines the variations in sensitivity due to orientation,
2. It provides a sensitivity performance record to enable efficient quality assurance and follow up testing.

1.1.3 Quantifying sprinkler sensitivity

From both tests, it is known that the sprinkler is at ambient room temperature, T_a, at time t = 0, and it is known that the sprinkler reachs its nominal operating temperature, T_{ACT} at time $t = t_{act}$ (activation time).

Based on the shape of the curve by which a body takes on or loses heat to its environment, the time constant can be determined. Under the rate of rise test, where the temperature of the environment is constantly increasing, the time constant is the amount of time by which the body lags behind its environment after some initial period of time equal to approximately four times the time constant (Fig. 1.2). However, under the plunge test condition where the temperature of the environment is constant, the time constant is effectively the amount of time necessary for the body to move 62.8 percent of the way to the temperature of its heated environment (Fig. 1.3).

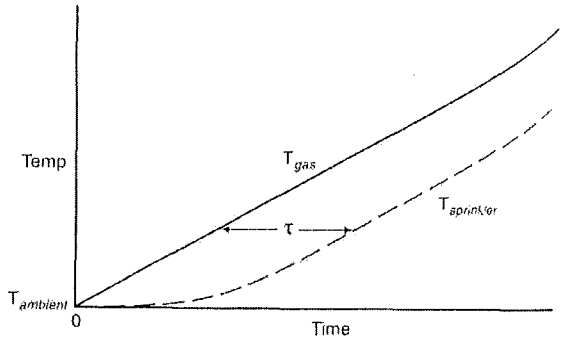

(Adopted from ref [9])

Figure 1.2 Representation of time constant for constantly increasing temperature environment

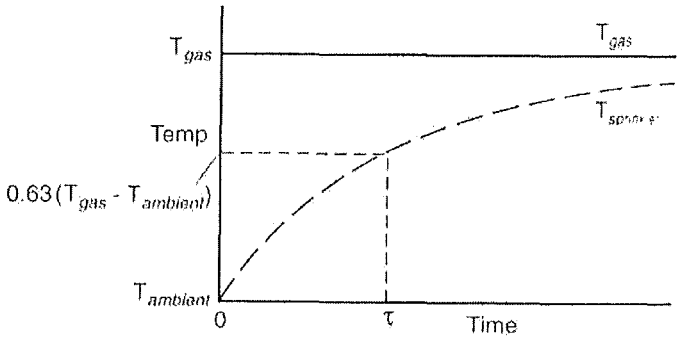

(Adopted from ref [9])

Figure 1.3 Representation of time constant for constant temperature environment

Definitions:

Time constant, τ: Time constant is a measure of the thermal sensitivity of a body and is defined as:

$$\tau = \frac{mc}{h_c A}$$

where

m = mass of the body,

c = specific heat of the body,

h_c = convective heat transfer coefficient, and

A = area of the body exposed to gas flow.

Often, the time constant cannot be determined readily for any specific body owing to the difficulties in estimating the convective heat transfer coefficient, as this varies with the velocity of the gases that pass by the body. As such, it is not a particularly useful term.

A new term, called "response time index" (RTI) was developed by the Factory Mutual Research Corporation (FMRC) to give a more meaningful measure of thermal sensitivity because it is independent of velocity. Since it was observed that the heat transfer coefficient of blunt bodies is roughly proportional to the square root of the gas flow velocity, it could then be eliminated by multiplying the time constant by the square root of its corresponding velocity;

$$RTI = \tau\, u^{1/2} = \text{constant}$$

Note that the above RTI does not take into account the complexities of conduction losses from the sprinkler head to the sprinkler frame, fittings and water in the adjacent piping. As such, the FMRC has reviewed the original RTI concept and introduced a modified model, "virtual RTI", which incorporates a conductive heat loss factor.

$$RTI_v = \frac{RTI}{\left(1 + \frac{C}{u^{1/2}}\right)}$$

where

C = conductivity factor.

The virtual RTI concept can be used successfully whenever the gas velocity is fairly constant, or does not change rapidly with time. It also assumes that the sprinkler fitting is initially at

ambient room temperature and that the conductive heat loss rate is proportional to the temperature rise of the sprinkler operating element.

1.2 Smoke detectors

Despite the recent introduction of new technologies, the vast majority of smoke detectors sold and in service today are based on either the photoelectric or the ionisation principle. In the twenty-five years since smoke detectors began to attain widespread acceptance as essential life safety fire protection devices [17], it has become generally accepted that "ionisation smoke detection is more responsive to invisible particles (smaller than 1 micron in size) produced by most flaming fires" [18]. It is also generally accepted that photoelectric detection is "more responsive to visible particles (larger than 1 micron in size) produced by most smouldering fires", "somewhat less responsive to smaller particles typical of most flaming fires", and "less responsive to black smoke than lighter coloured smoke" [18]. However, the relative merits of the two detector types continue to be a subject of discussion [19].

Presently, there are many approaches used in predicting the activation time of smoke detectors. The most commonly accepted engineering approach is to use a temperature correlation, which was originally proposed by Heskestad and Delichatsios in 1977. Specifically, activation for a 13 °C temperature rise at the detector location was selected from a set of experimental results for different detectors and fuels for which the results varied over a wide range [20]. However, recent literature has suggested that temperature rise at activation values of 4 °C or 5 °C provide good agreement with experiments in which current detectors were installed on ceilings of normal 2.4 m heights [21]. Furthermore, the assumptions inherent in the 13 °C temperature correlation are not always justified [21]. Both ionisation and photoelectric detectors are known to exhibit significant differences in response to different fuels and to smoke that has been "aged" [1] as it travels from the source. The fact that the temperature correlations do not capture any of these known differences make it limited in supporting the selection of the most appropriate smoke detection for a specific hazard.

Heskestad had also proposed a "simple model for (smoke) detector response" defined as L/u_e [22], where L described as the characteristic length, exists as a function of the aerodynamics of the device that relates to the ease with which smoke flows into the housing and enters the sensing chamber, and u_e is the flow velocity external to the detector. These parameters are independent of the properties of the smoke to which the detector is responding. However, it has been found that this model is only adequate at sufficiently high velocities. From the low velocity experiments performed in previous studies, it was found that a single characteristic length is insufficient to model the time response of spot-type detectors over the full range of conditions to which they are exposed.

As such, the "Critical Velocity Concept" is introduced, where it is hypothesized that there should exist a critical ceiling-jet velocity in the detector's region. Below this ceiling-jet velocity, smoke cannot reach the sensing chamber in sufficient quantity to cause an alarm, even when the optical density outside the detector exceeds the alarm threshold. This phenomenon has been reported by Bright [23] where smoke detectors were found not to respond at very low air velocities owing to the difficulty of aerosol entering their housing, even though the same detectors would respond at higher velocities. This suggested that there may be a design method which is based on the ceiling-jet velocity at various radii from the plume centreline, as a function of heat release rate and ceiling height above the fire.

1.2.1 Smoke detector tests

Many tests have been conducted in the past to determine the ability of detectors to satisfactorily sense the presence of a fire and their activation time. Among these tests are;

1 UL 217 [1] and UL 268 [2].

These tests are performed by Underwriters Laboratory, which utilizes a 1.7 m long x 0.5 m wide x 0.5 m high test chamber into which smoke is introduced. Detectors are mounted at the top of the chamber, and smoke-laden air is forced to flow past the detectors at about 0.16 m/s

[1] As particulates age, they coagulate, decreasing the number of particles while increasing the average particle size.

using a fan. The smoke concentration is controlled to produce an optical density between 0.003 m^{-1} and 0.2 m^{-1}. This smoke is produced from a cotton lamp wick and kerosene lamp.

2 UL 268A [3].

This is another test performed by Underwriters Laboratory, which uses a wind tunnel to simulate flow through a 0.3 m^2 duct at speeds between 0.1 m/s to 1.7 m/s. The smoke is produced by heating wood sticks on a hot plate and by burning a small pool of heptane.

3 Factory Mutual Smoke Detector Standard [4].

The standard outlines a series of tests performed by Factory Mutual in developing the smoke detectors standard. Smouldering cotton rope is used as a smoke source in theses tests. In order to pass the tests, a detector must activate before the smoke obscuration reaches 0.12 m^{-1}.

4 EN 54 [5].

This standard is developed by the European Committee of Standardization, which outlines a series of guidelines to how smoke detectors are to be tested in the European Community.

One of the major problems for smoke detector sensors is to distinguish the particles originating from an unwanted fire (smoke) and from nuisance aerosols in order to avoid nuisance alarms, because the worth of a smoke detector is determined by its ability to do so. Unfortunately, none of the tests above deal with air-borne particulates formed from other than flaming or smouldering fires, except UL 217 [1].

The fire-emulator/detector-evaluator (FE/DE) developed by the National Institute of Standards and Technology (NIST) [6] has been used to examine the response of smoke detectors to smoke and non-threatening nuisance aerosols such as dust, oil, water and etc.

1.2.2 FE/DE

The FE/DE is used to determine the response of spot-type detectors to physical products (temperature, gases and smoke) formed in simulated fires, as well as the response to stimuli not associated with a fire threat which could be present adjacent to an installed detector. It compares the analogue output of the detector's sensor measured as a function of aerosol (type, concentration, air flow) to the response of the detector to a flaming fire, and to the extinction of laser light in the FE/DE test section at optical densities up to 0.12 m^{-1}.

The FE/DE consists of a wind tunnel, designed to reproduce the time varying speed, temperature and concentration (gas and particulate) expected in the plume above the early stages of a fire (Fig 1.4). It has a test section 0.3 m high and 0.6 m wide. It has a variable speed fan and heater for the purpose of controlling the velocity and temperature ranges from 0.02 m/s to greater than 1 m/s and 20 °C to 80 °C respectively. A honeycomb flow straightener is placed in the tunnel before the test section to calm the flow.

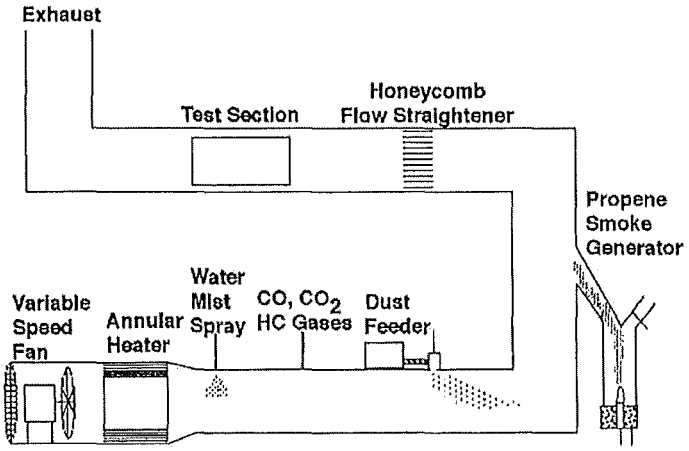

(Adopted from ref [12])

Figure 1.4 Schematic of fire-emulator/detector-evaluator (FE/DE).

Air temperature and velocity are measured at the test section using and thermocouples and hot-wire anemometer respectively. The hot-wire anemometer is calibrated to measure velocities ranges from 0.05 m/s to 5 m/s.

Laser light extinction is measured across the duct at the height of the detector inlet slightly forward of the detector placement and at the mid-height of the duct, as shown in Fig 1.5. The laser is reflected off two mirrors inside the tunnel to extend the path length to 1.5 m. Smoke deposition on these mirrors produces a slight positive baseline drift, which depends on the smoke concentration and test time. A He-Ne laser at 633 nm wavelength is used to measure the extinction. The signal-to-noise ratio is approximately 10^4:1 with no aerosol present. The signal is normalized by the pre-test signal level and recorded as a relative intensity ratio at 1 s interval.

The NBS aerosol generator [7] is used to produce the oil-based aerosols and inject them into the FE/DE. Peanut oil is used for the aerosol to simulate a nuisance cooking source. Small clay particles (7 mm nominal diameter), are added to the air flow using a variable speed screw-feeder fitted with a vibrator to simulate nuisance dusts. A small air jet is passed by the entrance tube to ensure even distribution of the dust across the duct.

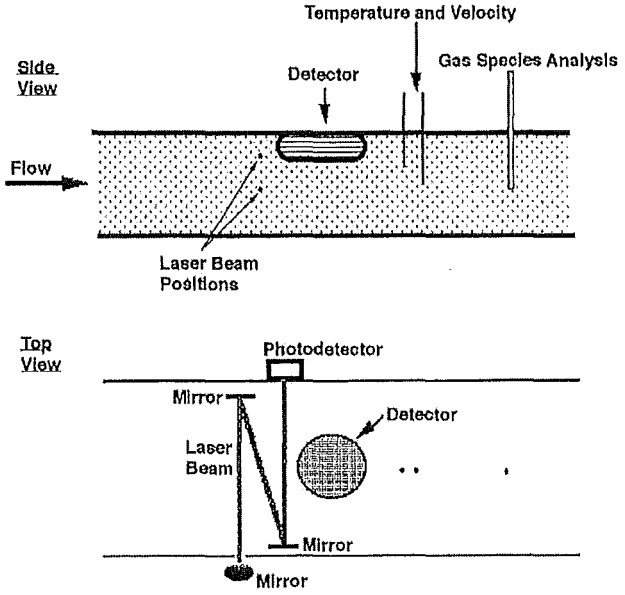

(Adopted from ref [9])

Figure 1.5 Schematic of FE/DE test section

A propane diffuser burner is used to provide a black smoke (soot) source. The smoke generator is operated between a range of fuel flow and co-flowing air of 0.3

cm^3/s to 25 cm^3/s and 500 cm^3/s to 1700 cm^3/s, respectively. A portion of the flow from the smoke generator is injected into the flow upstream the test section to achieve the desired smoke concentration. Step changes in smoke concentration up to 20%/m can be achieved. Details of the FE/DE can be found in ref. [8].

The FE/DE experiments begin by recording for 30 s the background signal from the smoke detector and from the laser system with clean air flowing through the test section at the predetermined temperature and velocity. Depending on the nature of the experiments, either the flow from the smoke generator, the dust feeder or the oil mist generator are initiated. The data are recorded every 3 s during the initial build up of aerosol concentration and for a 60 s steady-state condition. The aerosol flow is then terminated and measurements continued until the reference laser experiences close to full transmission and the detector signals fall to zero.

2. Wind tunnel

2.1 Scope

The original intentions of this research were to construct a bench-scale wind tunnel and conduct various tests on sprinklers and smoke detectors using the wind tunnel. The tests to be conducted included rate-of-rise test and plunge test for sprinklers, and FE/DE for the smoke detectors.

However, due to several unforseen circumstances, which caused the delay in the construction of the wind tunnel, as well as the selection and delivery of the fan, the project's objectives were re-evaluated, and were limited to only the construction of the wind tunnel.

2.2 Types of wind tunnel

There are two basic types of wind tunnels configurations.

The first basic tunnel type is an open-circuit tunnel (Fig 2.1). In this type of tunnel the air follows a straight path from the entrance through a contraction to the test section, followed by a diffuser, a fan section, and an exhaust of the air (suction type). Another type of the open-circuit tunnel, the blow type has the fan located before the test section.

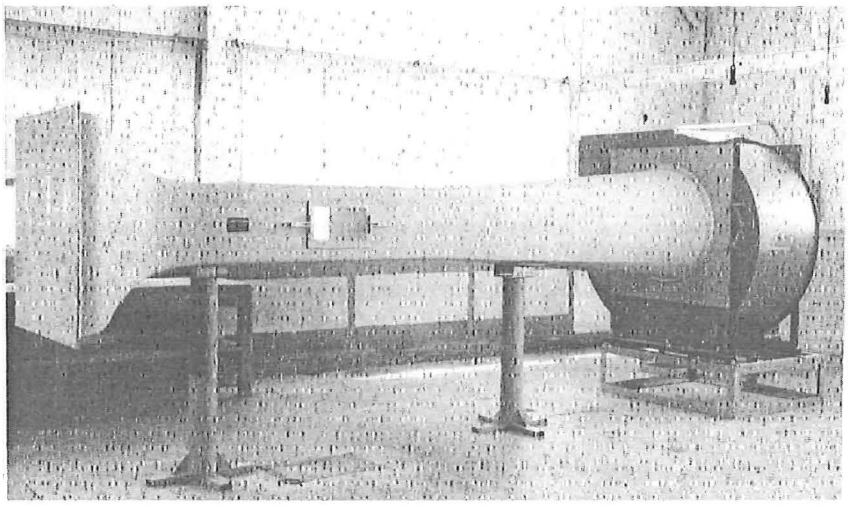

(Adopted from ref [15])

Figure 2.1 A typical layout of an open-circuit wind tunnel.

The second basic type is a closed return wind tunnel (Fig 2.2). This tunnel has a continuous path for the air. The great majority of the closed-circuit tunnels have a single return, although tunnels with both double and annular returns have been built.

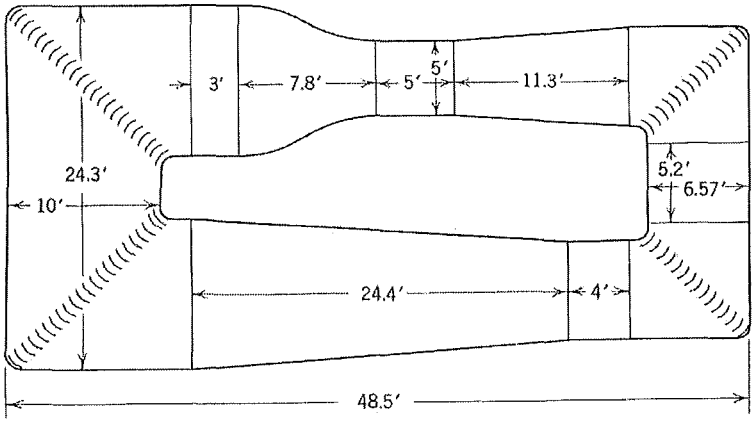

(Adopted from ref [14])

Figure 2.2 A typical layout of a closed return wind tunnel.

As with any engineering design, there are advantages and disadvantages with both the open and closed circuit type tunnels.

An open-circuit tunnel has the following advantages and disadvantages:

Advantages

1. Construction cost is less.
2. If one intends to do a flow visualization via smoke, there is no purging problem if both inlet and exhaust are open to the atmosphere.

Disadvantages

1. If located in a room, depending on the size of the tunnel to the room size, it may require extensive screening at the inlet to get a high quality flow. The same may be true if the inlet and/or exhaust is open to the atmosphere, when wind and cold weather can affect operation.

2. For a given size and speed the tunnel will require more energy to run. This is usually a factor only if used for developmental testing where the tunnel has a high utilization rate.
3. Noisy.

A closed return tunnel has the following advantages and disadvantages:

Advantages

1. Through the use of the corner turning vanes and possibly screens, the quality of the flow can be easily controlled.
2. Less energy is required for a given test section and velocity. This can be important for a tunnel used for developmental testing with high utilization.
3. Less noise when operating.

Disadvantages

1. Higher initial cost due to return ducts and corner vanes.
2. If used extensively for smoke tests, there must be a way to purge the tunnel.
3. Requires cooling due to the temperature rise as a result of pressure rise from the recirculating air.

3. Wind tunnel design

The initial idea for the wind tunnel design was to be able to recirculate the airflow in a loop. There were two reasons for this:

1. To minimise the power required for the heating element to heat the air up from ambient to 300 °C for the plunge tests.
2. To recirculate the smoke during the smoke detectors tests.

Even though the construction cost of a closed-circuit wind tunnel is higher, it offers advantages as described in the earlier chapter, such as low noise level, and low operating cost, which would be justified once the wind tunnel is in operation.

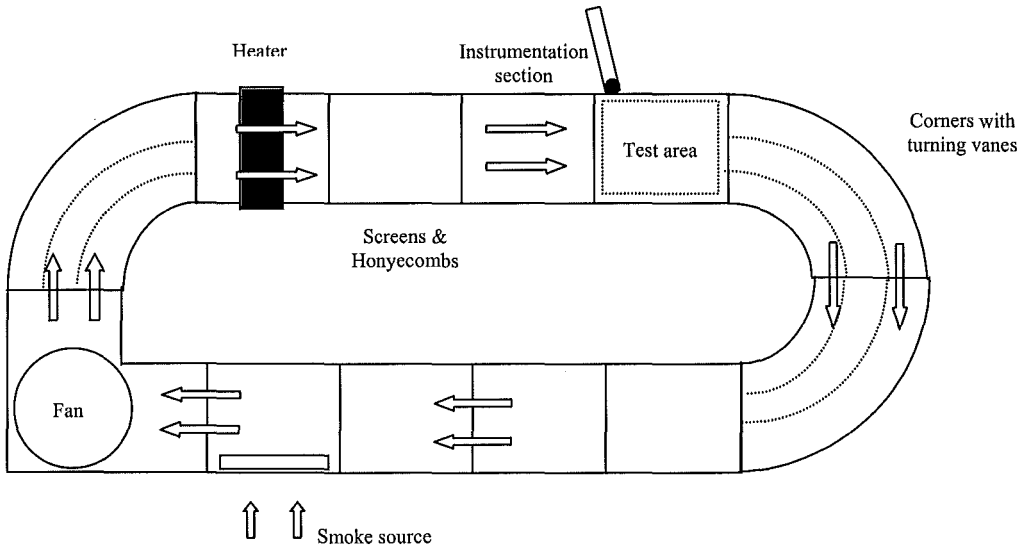

Figure 3.1 Sketch of the initial wind tunnel design

Fig. 3.1 shows a sketch of the initial wind tunnel design. Generally, the wind tunnel is made out of square cross-section ducts, connected by four corners to form a closed-loop. The corners are fitted with turning vanes to ensure smooth airflow around the bend, thus minimising the pressure loss.

The electrical heating element is used to heat the air from ambient to approximately 300 °C for the purpose of sprinkler testing.

Wire mesh screens and honeycombs are placed between the fan and the test section for the purpose of flow straightening because it is very important that the airflow be relatively laminar across the test section to ensure that the tests can be done properly. Since air discharged from the fan is generally turbulent in nature, it is therefore necessary to straighten the airflow before it enters the test section.

Instruments such as thermocouples, velocity probes and laser are to be fitted prior to the test section to ensure that the desired volume flow and operating temperature is achieved. The laser is used to determine the optical density of smoke during the smoke detector tests. Sampling ports are located before and after the test section to determine the species concentration of the smoke.

One side of the test section is to be fitted with a window for viewing purposes. The topside of the test section will be fitted with an access door for insertion of test subjects (sprinkler heads and smoke detectors).

An access door is fitted along the return passage to introduce the smoke into the loop.

Ideally, a diffuser should be used after the fan to reduce the airflow speed (Fig. 3.2). The gradual expansion would also aid in reducing the turbulence. A well-designed contraction following the diffuser would speed up the airflow, and create a uniform and parallel flow at the exit. This should minimise the unsteadiness and degree of turbulence of the airflow in the test section. Screens and honeycombs should be placed between the diffuser and contraction, where the airflow is slowest so that the pressure losses across them are at a minimum.

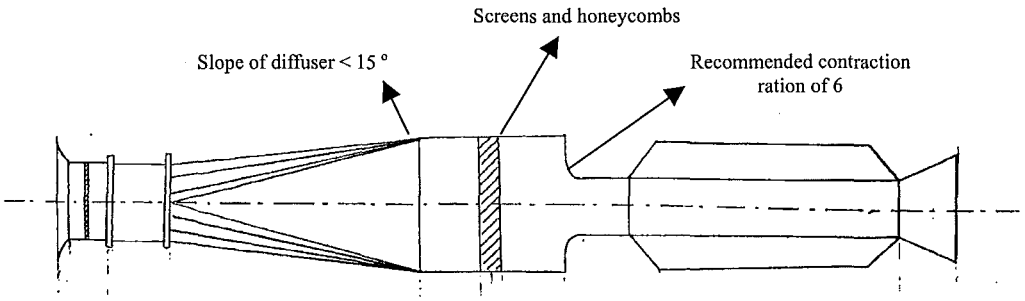

Figure 3.2 Ideal design for the wind tunnel (diffuser and contraction)

In order to prevent any flow separations, the recommended slope for a diffuser is no greater than 15°, and the recommended contraction ratio for a contraction is 6. To meet these recommendations would require a large space, and therefore it was decided to use only straight ducts as illustrated in Fig. 3.1 despite the advantages of using the diffuser and contraction. The trade-off for the space saving is to increase the number of screens to be used to straighten the airflow, but this would in turn lead to an increase in the pressure losses. Therefore, balancing the system once the wind tunnel is being fabricated is a very crucial task.

3.1 Design parameters

The design criteria for the wind tunnel were as followed;

1. It had to be inexpensive.

   The resources that were available for the construction of the wind tunnel were fairly limited. Because the wind tunnel is only intended mainly for academic and research purposes, financial assistance from outside was unavailable. Therefore the wind tunnel had to be built with the least possible cost, while achieving an acceptable level of performance required.

2. It had to be completed in a short period of time.

   The wind tunnel was expected to be built within a 4 to 6 week period because times must be allocated to the testing and commissioning of the wind tunnel, instrument calibration and the tests as well.

3. Air velocity up to 2.5 m/s is required at the test section.

   FE/DE test requirement.

4. The airflow at the test section must be relatively laminar to simulate the ceiling jet in actual fire condition.

5. Smoke is to be injected into the wind tunnel.

   Smoke detector test requirement.

6. The maximum temperature of the airflow at the test section must be approximately 300 °C.

   Plunge test and rate-of-rise test requirement.

7. Lab dimensions.

   The wind tunnel will be located in a new laboratory, which is yet to be constructed within the Civil Department Laboratory wing. Although the exact dimensions of the new laboratory are not known, the wind tunnel's size should not be excessive (i.e. > 3 m).

3.2 System components (Background Information)

No single wind tunnel is adequate for all possible tests. The first step in the design of the tunnel is to determine the size and shape of the test section. The cross sectional area of the tunnel test section basically determines the overall size of the facility. The test section size, speed, and design will determine the required power. The size of the facility will determine the structural or shell costs, and the power and operating hours will determine the energy portion of the operational cost. Often, there is a balance between initial costs and operating costs for a design. A tunnel's circuit length may be cut short to hold down the initial costs, but higher energy costs of operation may incur. Thus the trade off between the two are examined carefully.

3.2.1 Test section

This is the starting point in the design of a wind tunnel. The purpose of a wind tunnel is to provide a uniform and controllable airflow in the test section that passes over the subject being tested.

Over the years many shapes have been used for test sections, such as round, elliptical, square, rectangular, rectangular with filleted corners etc. The cost and power are directly determined by the cross sectional area. The difference in losses in the test section due to the tunnel shape is negligible [14]. Therefore the shape of the test section should be based on utility and aerodynamic considerations.

3.2.2 Heating elements

There are many ways in which air may be heated. However, it was decided in this application that heating element is to be used as the heating source. Electrical energy is transformed into heat in open wire spirals, strips or sheathed wires elements strung across the path of the airflow through the heater casing so that the system is a form of direct air heating.

Since a temperature difference is required to cause the heat to flow from the wire to the air stream, the wire temperature will rise, and furthermore the ultimate temperature of the wire will increase as the airflow velocity is reduced. The ultimate temperature allowable is limited by the material from which the wire is made and the life expected from it.

Manufacturers of resistance heating wire commonly quote the surface temperature reached by various gauges of wire under nominal operating conditions (i.e. current, temperature and airflow velocity). In practice, the temperature rise will be increased by concentrating the wire into a small space, by spiralling, and decreased by the forced convection effect or an air stream. Therefore practical tests are usually necessary in order to determine the rating of the elements for the temperature required.

Note that it is necessary to check that the wire does not immediately reach softening or fusing temperature should the airflow be accidentally interrupted, because under these circumstances, the full heating load is supplied continuously, but is not removed by the airflow, thus causing the casing to reach an excessive temperature rapidly. Therefore protection should be provided in the form of a switch to interrupt the current before a dangerous temperature is reached.

As far as the airflow is concerned, the heating element is considered as obstruction. Therefore, a pressure drop across the element is anticipated when the airflow is passing through the element. Since the pressure drop across the element varies for different designs, the individual manufacturer should be consulted.

3.2.3.1 Convection

Heat always tends to flow from a hot to a cold body. The function of the heating element is to achieve a continuous heating of an air stream (or other gas) to the desired temperature. Generally, there are three natural processes of heat transfer involved, radiation, conduction and convection. However, only the convection heat transfer mechanism is of practical significance for the present purpose.

Convection implies the continuous movement of successive masses of air to and from a hot surface where heat is taken up (strictly the first state of the convection process takes place by conduction across a thin film of gas which never leaves the surface). There are two types of convective heat transfer mechanism, I) Forced convection, and II) Free or natural convection.

Definitions of convective heat transfer mechanism:

Forced convection: The heat transfer mechanism, which is deliberately promoted by placing the hot surface in the airflow from an external influence, such as a fan is termed forced convection.

The general form of convective heat transfer equation appropriate for forced convection is:

$$Nu_x = C\,\mathrm{Re}_x^{\,m}\,\mathrm{Pr}^n, \quad \left(\mathrm{Re}_x = \frac{\rho U x}{\mu}, \quad \mathrm{Pr} = \frac{c_p \mu}{k}\right)$$

where

C, m and n = constant,

Nu_x, Re_x and Pr = dimensionless groups,

x = characteristic dimension (m),

U = airflow velocity (m/s),

ρ = air density (kg/m^3),

c_p = specific heat (kJ/kg.K),

k = thermal conductivity (kW/m.K).

For flow normal to the outside of a cylinder, the empirical relationships have the general form;

$$Nu_{d,f} = C\,\mathrm{Re}_{d,f}^{n}\,\mathrm{Pr}_{f}^{1/3}$$

in which the coefficient C and the index n depend on both the Reynolds number (for which the outside tube diameter is used as the characteristic dimension) and the geometry of the tube layout (i.e. number of tube rows; successive tubes in-line or staggered).

Refer to *Appendix 2* for the use of the above equations in this application.

Free convection: The convective heat transfer mechanism due to the tendency of heated air, being less dense, to rise and make room for fresh, cold air is termed free or natural convection.

Since the primary heat transfer mechanism in this application is of the forced convection type, details of free convection will not be discussed. It is recommended that the reader refer to the appropriate heat transfer text for more detailed discussion on free convection.

3.2.3 Corners

Closed-circuit tunnels need corners with guide vanes of some kind to deflect the flow without the boundary-layer separations (to avoid large losses) that normally occur in all but very gentle bends. The "first corner" is the first one downstream of the test section, and so on. Corners are usually of constant area. The shape of the vanes varies from bent plates to highly cambered airfoils.

There are a variety of corners available; (i) Full radius corner (Fig 3.2), (ii) Short radius vaned corner (Fig. 3.3), and (iii) Vaned square corner (Fig. 3.4).

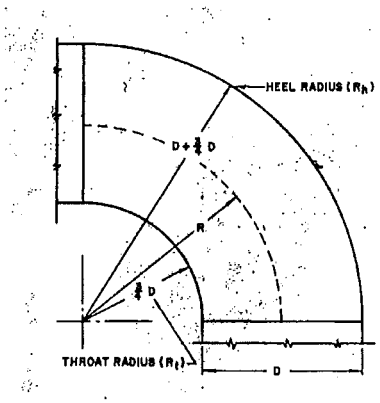

(Adopted from ref [26])

Figure 3.2 Full radius corner

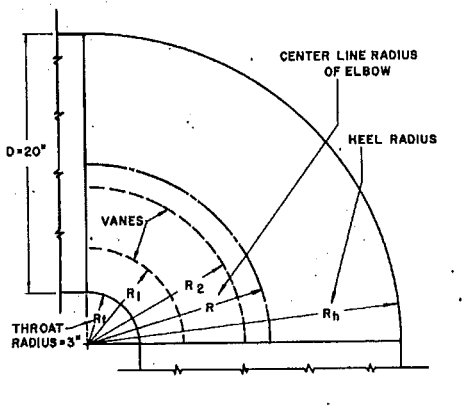

(Adopted from ref [26])

Figure 3.3 Short radius vaned corner

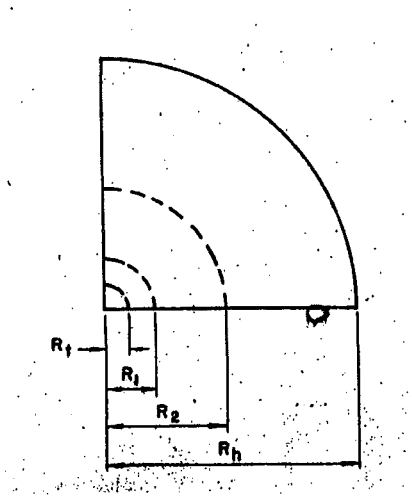

(Adopted from ref [26])

Figure 3.4 Vaned square corner

Full radius corners (Fig 3.2) are constructed with a throat radius equal to ¾ of the duct dimension in the direction of the turn. A corner having this throat radius has an R/D ratio of 1.25. This is considered to be an optimum ratio.

The short radius vaned corners (Fig 3.3) can have one, two or three turning vanes. The vanes extend the full curvature of the corner and their location is determined from the following chart.

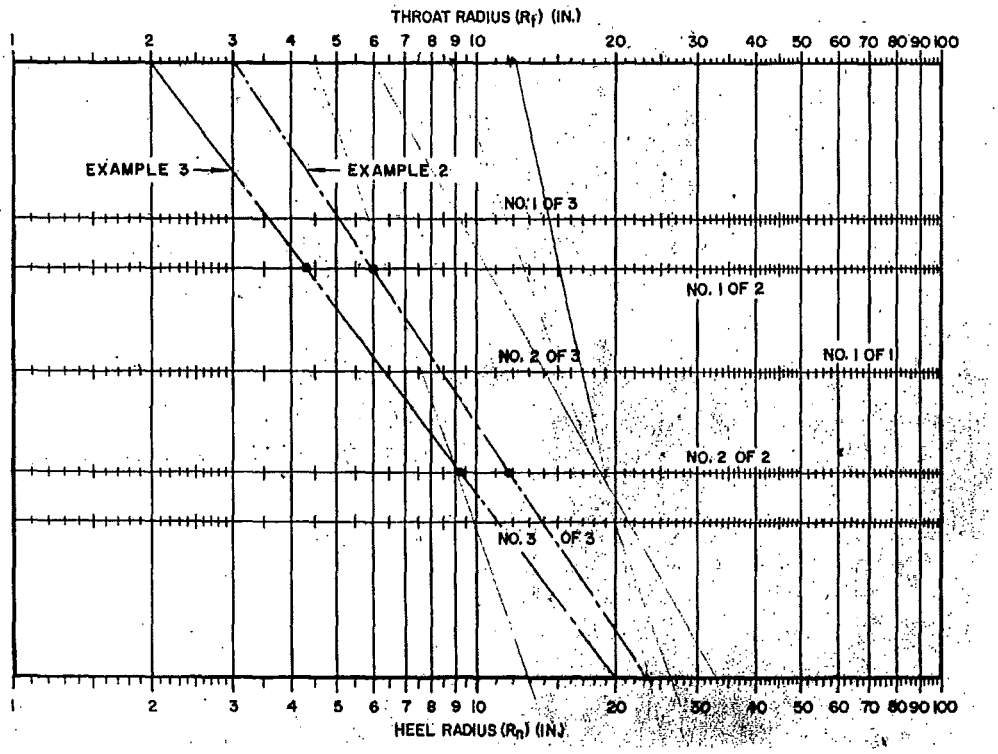

(Adopted from ref [26])

Chart 1 Vane location for rectangular ducts

A vaned square corner has either double or single thickness closely spaced vanes (Fig 3.4). These corners are used where space limitation prevents the use of curved corners and where square corners are required. The vaned square corner is expensive to construct and usually has a higher pressure drop than the vaned short radius corner and the full radius corner.

3.2.4 Screens and honeycombs

Turbulence in the test section can generally be reduced by the installation of screens and honeycombs upstream. Screens reduce the axial turbulence more than the lateral turbulence. Screens increase the required power of the tunnel owing to their relatively large pressure drop in the flow direction, which reduces the higher velocities more than the lower, and thus promotes a more uniform axial velocity. Honeycombs have small pressure drops and thus have less effect on axial velocities, but owing to their length, they reduce the lateral velocities. The minimum length of a honeycomb should be 6 – 8 times the cell size. Both screens and honeycombs reduce lateral and axial turbulence, probably due to an exchange in energy between the axis as the turbulence tends toward isentropic turbulence downstream.

A problem with screens is their ability to accumulate dust, especially when smoke is used. Thus the screen's porosity and pressure drop will change, which in turn will change the velocity and angularity distribution in the test section in an arbitrary way in time. Therefore, when screens are used, they must be installed so that they can be cleaned, and the quality of the test section flow must be monitored.

Screens used for turbulence reduction should have the projected open area to total area ratio, β, greater than 0.57. Screens with smaller ratios suffer from a flow instability that appears in the test section.

For screens, many of the turbulent reduction theories are based on a pressure loss coefficient K, defined as pressure loss across the screen ΔP divided by the mean flow dynamic pressure q. The relationship can be simplified to the following:

$$K = K_0 + \frac{55.2}{\mathrm{Re}_d}$$

When multiple screens are used, the pressure drop K is the sum of the individual screens. Multiple screens must have a finite distance between them so that the turbulence induced by the first screen damps out before the second screen.

Spacing values of 30 times the mesh size as well as 500 times the wire diameter have been suggested.

Strictly speaking, when screens are placed behind the honeycomb, the turbulence reduction is based on the turbulence behind the honeycomb and thus require a minor correction. This however, was not done for simplicity.

3.2.5 Fan

Before selecting a fan, certain basic information must be known, namely:

b) The quantity of air to be moved,
   - The quantity of air to be moved is obviously the first choice. Therefore, the fan selected must be able to supply the required airflow across the test section.

c) The pressure against which the fan is required to operate (static, velocity and total pressure),
   - When considering the pressure against which the fan must work, the problem arises as to whether selection should be made on the basis of total pressure or static pressure. Strictly speaking, the total pressure should be used to calculate the system resistance, and thus for the selection as it gives a better indication of the fan's capabilities. But to do this requires the knowledge of both the fan size and the nature of connections between the fan and the tunnel. Since these dimensions are often not known prior to the selection, static pressure shall be used as the basis of selection.

d) The density of the air or gas to be moved.
   - Often, fan tables and curves are based on air at standard atmospheric conditions. If a fan is to operate at non-standard conditions, the selection procedure must include a correction.

Additional information such as noise, vibrations, type of motor and power supply etc. may be considered when making the final decision.

Definition of pressures:

Static pressure: When moving matter meets resistance, its progress is retarded and air is no exception. Even straight ducts restrict its flow, due to friction against the sides. As resistance increases flow decreases unless greater pressure is put behind it. For instance, for a duct with a generous size with free outlet, air will flow through easily. The pressure which sets it in motion will produce velocity without building up internal pressure. If however, the resistance of the duct is increased, the flow will be reduced. That will cause pressure to build up within the duct. The flow will then depend on the amount of internal pressure developed. The pressure, which is not produced by velocity, but is the pressure which maintains the velocity against resistance, is called static pressure.

Velocity pressure: Airflow is produced by a difference in pressure between two points (high pressure to low pressure). Its rate of flow depends on the resistance met with by the air stream. Like everything else that moves, air exerts pressure against obstructions in relation to its speed, and this pressure is called velocity pressure.

Total pressure: The static pressure developed by a fan is the pressure it can build up in order to move air against resistance. In other words, it is its potential ability to do work. In all air movement, there is some static pressure and some velocity pressure according to the resistance. The sum of the two represents the total pressure developed by the fan and is called the total pressure.

3.2.5.1 Types of fans

Generally, fans are identified by two general groups:

1. Centrifugal, in which the air enters axially, turns at right angles through the impeller and is discharged radially (Fig 3.5).
2. Axial, in which the air flows axially through the impeller (Fig 3.6).

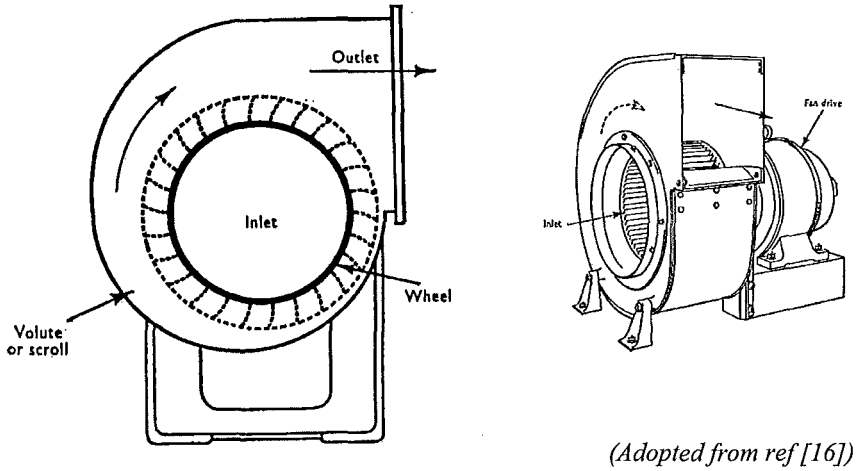

(Adopted from ref [16])

Figure 3.5 General layout of a centrifugal fan

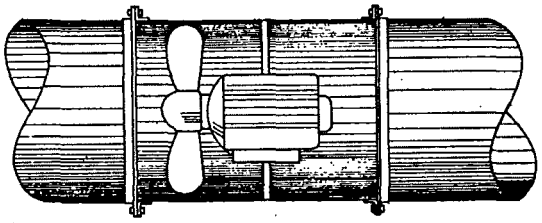

(Adopted from ref [26])

Figure 3.6 General layout of an axial fan

Centrifugal fans are used in most applications because of their wide range of quiet, efficient operation at comparatively high pressures. Furthermore, airflow can be varied to match the system requirements by simple adjustments to the fan drive or control devices.

Centrifugal fans can be further classified into three different types according to blade configuration:

1. Straight radial blades,
2. Forward-curve blades, and
3. Backward-curve blades.

Each type has its own application range and limits. The shape of the blades influences the force exerted on the air and the proportion of energy imparted in the form of velocity. The velocity of air leaving the impeller is proportional to the length of arrows in Fig. 3.7.

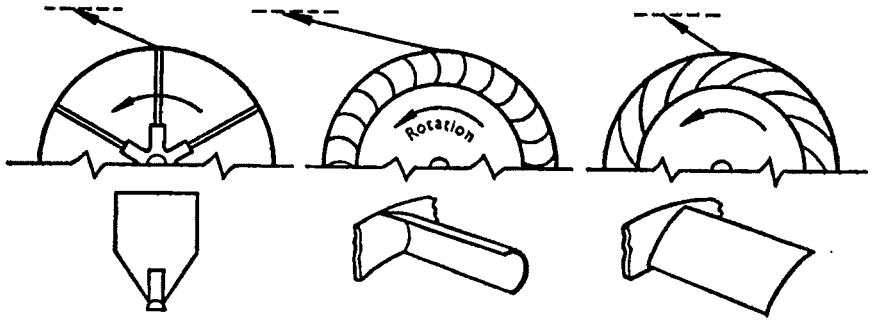

(Adopted from ref [16])

Figure 3.7 Types of centrifugal fan blades

The efficiency of centrifugal fans suffers from the fact that air handled must turn through 90 °. This causes losses of energy due to shock and eddies. Moreover the aerodynamic efficiency of the scroll is generally rather low. The fan efficiencies are usually between 45 % and 85 % according to type.

Axial fans are excellent for large air volume applications where higher noise levels are of secondary concern. Usually, these fans require guide vanes to obtain the best efficiencies when operating against pressures considered normal for centrifugal fans. However, these fans may be applied without guide vanes.

Fig. 3.8 illustrates the approximate sound power level of a typical centrifugal fan and an axial fan. The frequencies detectable by the human ear (300 to 10,000 cycles per second) are the least favourable for the axial fan. Therefore, to obtain acceptable sound levels with the axial fan, sound attenuation may be required.

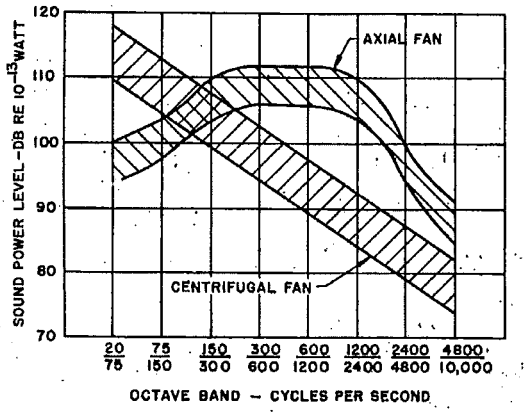

(Adopted from ref [26])

Figure 3.8 Approximate sound power levels of a typical centrifugal and axial fan.

The performance of a typical centrifugal fan and an axial fan can best be compared using the specific speed concept. Specific speed is a fan performance index based on the fan speed, capacity and static pressure. Fig. 3.9 shows the ranges of specific speed in which six types of centrifugal and axial fans operate at high static efficiencies. The figure indicates that forward-curved blade centrifugal fans attain their peak efficiencies at low speeds, low capacities and at high static pressures. However, propeller fans reach high efficiencies at high speeds and capacities and low static pressures.

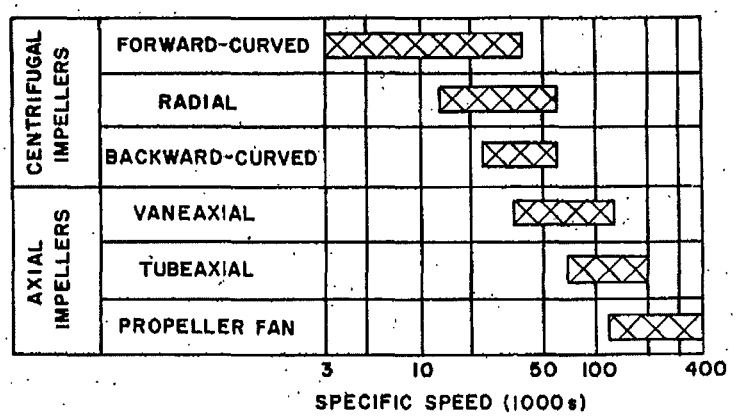

(Adopted from ref [26])

Figure 3.9 Specific speed ranges for centrifugal and axial fans

3.2.5.2 Fan performance

Fans are selected to give a certain quantity of air against a certain pressure and their performance must be defined largely by these two factors. Although designed for optimum performance at a given duty, a fan is capable of working quite reasonably over a range of pressures and volumes, and its performance is more completely defined by a graph of pressure and volume flow of air, known as the "characteristic curves" of the fan (Fig 3.10).

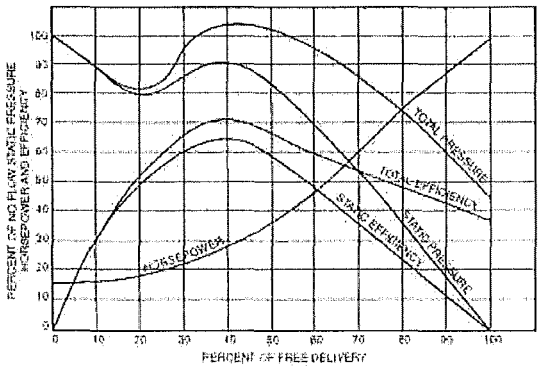

(Adopted from ref [27])

Figure 3.10 An example of a fan's characteristic curves

Pressure Volume Curve

Figure 3.11 and 3.12 shows a typical static pressure curve for an axial and centrifugal fan.

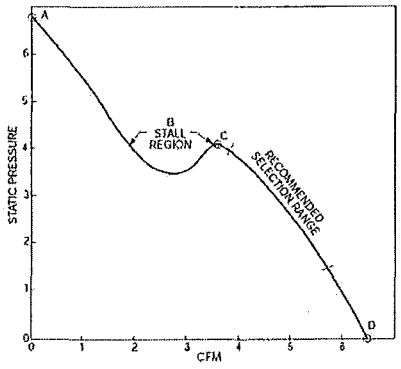

(Adopted from ref [27])

Figure 3.11 Static pressure curve, axial

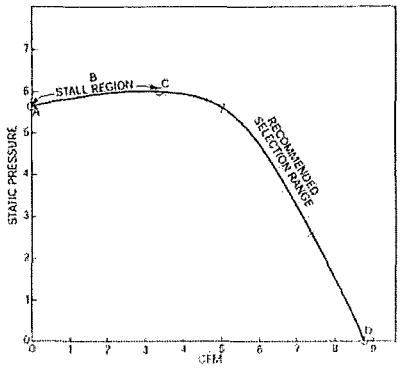

(Adopted from ref [27])

Figure 3.12 Static pressure curve, centrifugal

Point A represents the point of zero airflow on the static pressure curve. It is frequently referred to as "block off," "shut off," "no flow," and "static no delivery."

Point B depicts the stall region of the static pressure curve. Operation in this area is discouraged because of erratic airflow that generates excessive noise and vibration.

Point C depicts what is referred to as the peak of the static pressure curve, and point D is the point of maximum airflow.

Curve segment CD is often referred to as the right side of the fan curve. This is the stable portion of the fan curve and is where the fan is selected to operate. Curve segment AC is then considered to be the unstable portion of the curve.

The fan static pressure curve is the basis for all airflow and pressure calculations. For a given static pressure (SP), there is a corresponding volume flow rate (CFM) at a given speed (RPM). Simply locate the CFM required, and project a vertical line to the point of intersection on the static pressure curve. From the point of intersection, project a horizontal line to the static pressure scale to establish the corresponding SP at that particular RPM.

Brake Horsepower Curve

Having established a SP and CFM, an operating brake horsepower (BHP) can be established (Fig 3.13).

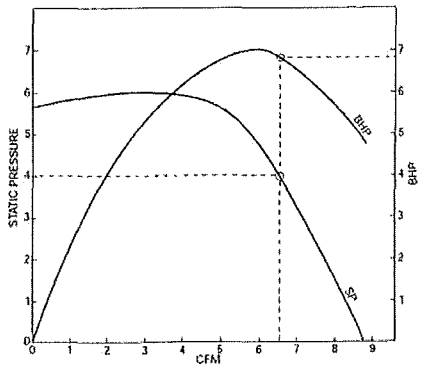

(Adopted from ref [27])

Figure 3.13 Static pressure/horsepower curve

The BHP is determined in a similar way as the static pressure.

Definition: Horsepower is defined as the power required to operate a fan. There are different kinds of power such as mechanical horsepower, electrical horsepower and brake horsepower.

Brake horsepower is the actual mechanical horsepower as developed at the pulley or coupling of a machine and measured

by a brake. It represents the actual power which must be applied to drive the fan and includes all losses.

Operating Point

With the static pressure curved established, it is now possible to determine the operating point by establishing the system line. Generally, the system line is simply a parabolic curve made up of all possible static pressure and airflow combinations within a given system, and is determined from the fan law that static pressure varies as RPM^2. By superimposing both curves upon a system characteristic as in Fig 3.14, there is only one point of intersection. This point is the only possible operating point under the conditions. If the fan speed is increased, the point of operation moves upward to the right. If the speed is decreased, the operating point moves down and to the left.

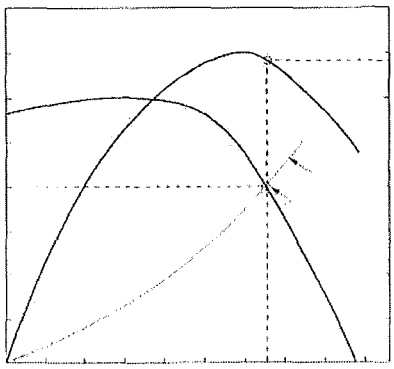

(Adopted from ref [27])

Figure 3.14 Fan/System Operating Point

Sometimes a fan system does not operate properly according to the design conditions. The measured airflow in the fan system may be deficient or it may be delivering too much air. In either case, it is necessary to either speed up or slow down the fan to attain design conditions.

Knowing that the fan must operate somewhere along the system curve, it is possible to predict the fan performance at other speeds by applying the following fan laws:

1. CFM varies as RPM
2. SP varies as RPM^2
3. BHP varies as RPM^3

Note: Refer to *Appendix 1* for more comprehensive details on fan laws.

Subsequently, the new "operating line" (SP and BHP) between various fan speeds can be graphically presented as shown in Fig 3.15. These speed changes represent an example of fan control that can be accomplished through drive changes or a variable speed motor.

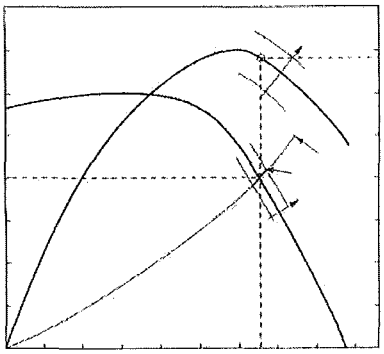

(Adopted from ref [27])

Figure 3.15 Variable Fan Characteristic Curve

Another way to present an "operating line" is to add a damper, making the system the variable characteristic. By modulating the damper blades, new system lines are created resulting in an operating line along the fan curve, as shown in Fig 3.16.

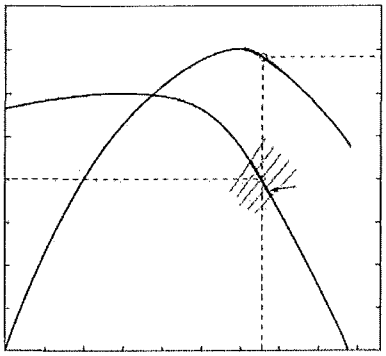

(Adopted from ref [27])

Figure 3.16 Variable System Characteristic Curve

Combining the fan control curve (Fig 3.15) with the system controlled curve (Fig 3.16) results in a fan/system controlled curve having an "operating region" as shown in Fig 3.17.

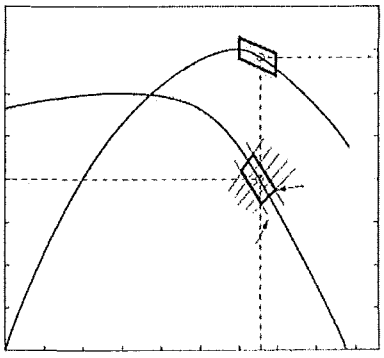

(Adopted from ref [27])

Figure 3.17 Variable Fan/System Characteristic Curve and operating region

3.2.5.3 Effect of density on fan performance

Performance tables and charts for fan are based on air at standard atmospheric conditions of 21 °C and 760 mm Hg barometric pressure. Therefore, if a fan is to operate in non-standard conditions, adjustments must be made to the fan's operating conditions. When the air density changes, the result is proportional to the change in power absorbed and in the pressure (static or total) developed by the fan at constant volume flow. These are demonstrated from the following fan laws:

1. Volume flow of air does not vary with change in density.
2. Pressure developed varies directly with change in density.
3. BHP absorbed varies directly with change in density.

Adjustment shall be done in the following way:

1. Obtain the air density ratio, where

$$\text{Air density ratio} = \frac{\text{density at new condition}}{\text{density at normal condition}}$$

2. Calculate the new fan static pressure by multiplying the given static pressure with the air density ratio.
3. Calculate the new BHP by multiplying the given BHP with the air density ratio.

Note that the volume flow remains unchanged since it does not vary with change in density.

If atmospheric corrections are ignored in the fan selection, fan speed and air capacity may be too small, and the BHP somewhat high.

3.2.6 System resistance

As previously mentioned, two essential facts must be known in order to select a fan to work on a system. The first is the quantity of air required; and secondly the pressure against which the fan must work, and is termed "system resistance." The second requirement can only be done when any system has been arranged and sized.

The system resistance depends on a number of things. For instance, less pressure is required to send a given amount of air through a large section as compared to a small section, which result in a slower flow at the larger section. A sharp right angle bend will be more difficult to negotiate than an easy, slow sweeping bend. Energy is lost at other places as well such as restrictions, expansions, heating elements, etc., all of which create back pressure to the fan.

3.2.8.1 Effect of density on system resistance

Like a fan's performance tables and charts, pressure drop across any fittings and restrictions is also based on standard atmospheric conditions. Therefore necessary adjustments must be made if the system is to operate in non-standard conditions.

3.2.7 Others (Thermocouples, velocity probes, laser transmitter/receiver)

In order to carry out the tests, instrumentation such as thermocouples, velocity probes and laser transmitter/receiver should be installed prior to the test section to ensure that the test conditions are met.

The testing and commissioning of the wind tunnel, is however outside the scope of this report due to reasons mentioned previously, and therefore will be done in the future.

4. Design considerations

Having considered various designs issues as mentioned in the previous section, it is now possible to select the components suited for the tasks. As previously mentioned, the first step in designing a wind tunnel is to determine the size and shape of the test section.

4.1 Test section

The design parameters at the test section are:

1. Maximum airflow velocity up to 2.5 m/s.
2. Maximum air temperature approximately 300 °C.

After careful consideration, it was decided to use a square test section, as this would provide a good representation of the actual orientation where sprinklers or smoke detectors are to be mounted. This is very important because the flat ceiling is able to provide the ceiling-jet so that the interaction between its velocity and the sprinklers and detectors could be investigated. Apart from that, a square section would provide advantages such as the ease of installation and conducting tests. Furthermore, the flat walls would allow easy installation of windows for viewing.

The dimensions of the test section were selected to be 300 mm x 300 mm. This was considered as appropriate as it would provide sufficient space between the test subjects and the wall to avoid any boundary problems.

As the air proceeds along the test section, the boundary layer thickens. This action reduces the effective area of the test section and causes an increase in velocity. The velocity increase in turn produces a drop in static pressure. Often, this issue can be solved by applying wall corrections. This, however was not done for simplicity purposes.

A larger section is not necessary since it would not improve the flow significantly, but rather increases the overall size of the wind tunnel, and also the

fan's power in achieving an equivalent volume flow. These would then lead to a higher construction and operating cost.

With the cross-sectional area of 0.09 m^2 (0.3 m x 0.3 m), the volume flow required at the test section is

$$Q = V \times A$$
$$= 2.5 \text{ m/s x } 0.09 \text{ m}^2$$
$$= 0.225 \text{ m}^3/\text{s}$$

4.2 *Initial estimate of system resistance*

Since the volumetric flow required has been determined, the next step is to estimate the pressure against which the fan must work (i.e. system resistance). Although the proper estimate can only be done when the wind tunnel design has been finalized, an initial estimate is necessary to give a rough idea on fan selection.

For consistency purposes, the loss factor method has been used to estimate the system resistance. This method details the loss of individual features of the system in terms of a loss of kinetic energy, i.e. velocity pressure from the airflow at the point under consideration. This assumes that for all rates of air flow, loss is proportional to $(\text{velocity})^2$. This method is justified in practice except for long straight ducts, which is not the case as far as the wind tunnel is concerned.

The loss factor, K will be seen to be that proportion of the velocity pressure at the section indicated which has to be supplied by the fan in order to ensure that the required quantity of air will pass through the feature or obstruction. The velocity pressure is taken from the average velocity at the section, i.e.

$$\text{average velocity} = \frac{\text{Volume flow}}{\text{Area of section}}$$

Great accuracy must not be expected in the calculation of the resistance of a system of ductwork, as manufacturing tolerances will preclude this. Generally an accuracy of ± 10 % may be regarded as being very good.

The following estimates are based on the initial sketch (Fig. 3.1).

Table 4: Initial estimate of the system resistance

Section		Dimension (mm)		Length (mm)	k	Velocity (m/s)	Velocity pressure (Pa)		Static pressure (Pa)		Total pressure (Pa)	
		W	D									
1	Elbow (R/D = 1.25)	300	300	2625	0.18	2.5	1.90	1.90	0.33	0.33	2.24	2.24
2	Heater	-	-	-	-	2.5	1.90	3.81	20.00	20.33	21.90	24.14
3	Straight	300	300	300	0.02	2.5	1.90	5.71	0.04	20.37	1.94	26.08
4	Straight	300	300	300	0.02	2.5	1.90	7.61	0.04	20.41	1.94	28.02
	Screens	-	-	-	1.0	2.5	1.90	9.51	1.94	22.35	3.84	31.86
5	Straight	300	300	300	0.02	2.5	1.90	11.42	0.04	22.39	1.94	33.80
6	Straight	300	300	300	0.02	2.5	1.90	13.32	0.04	22.42	1.94	35.74
7	Elbow (R/D = 1.25)	300	300	2625	0.18	2.5	1.90	15.22	0.33	22.76	2.24	37.98
8	Elbow (R/D = 1.25)	300	300	2625	0.18	2.5	1.90	17.12	0.33	23.09	2.24	40.21
9	Straight	300	300	300	0.02	2.5	1.90	19.03	0.04	23.13	1.94	42.15
10	Straight	300	300	300	0.02	2.5	1.90	20.93	0.04	23.17	1.94	44.09
11	Straight	300	300	300	0.02	2.5	1.90	22.83	0.04	23.20	1.94	46.03
12	Straight	300	300	300	0.02	2.5	1.90		0.04		1.94	47.98
13	Fan								**23.24**		**47.98**	
				TOTAL	**1.7**							

This value has been adjusted to include the effect of density

Please refer to *Appendix 4* for calculation details.

Note:

The column K represents the loss factor of each individual component. The following sections explain how these values are derived. Owing to the constant cross sectional area of the wind tunnel, the velocity is also constant, which results in a constant velocity pressure. The static pressure however, is different for different components since static pressure is a function of the loss factor and velocity pressure. The total pressure is the summation of static and velocity pressure. According to the initial estimate, the fan selected must be able to supply a static pressure of 23.24 Pa while be able to met the volume flow required.

4.2.1 Corners

The friction loss through the corners is expressed in terms of an additional equivalent length of duct, which is to be added to the straight run of duct to obtain the total equivalent length of duct. The straight run of duct is measured to the intersection of the centreline of the corners (Fig. 4.1).

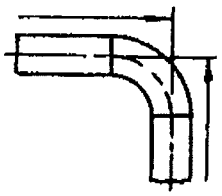

(Adopted from ref [26])

Figure 4.1 Guide for measuring duct lengths.

In order to determine the additional equivalent length of duct to be added to the straight run of duct of the corner, the centreline radius of the corner must first be determined. For instance, for a 300 mm x 300 mm corner, the recommended throat radius,

$$R_t = \frac{3}{4} \times D$$
$$= \frac{3}{4} \times 300$$
$$= 225 \text{ mm}$$

Thus the centreline radius is just the sum of the throat radius and half of the height of the corner,

$$R_{CL} = R_T + (\frac{1}{2} \times D)$$
$$= 225 + (\frac{1}{2} \times 300)$$
$$= 375 \text{ mm}$$

Thus the R_{CL}/D ratio,

$$R_{CL}/D = 375/300 = 1.25$$

This yields a L/D ratio of 7.5 for a rectangular vaned corner, with single vane. Thus the additional equivalent length,

$$\begin{aligned} L &= L/D \text{ x } D \\ &= 7.5 \text{ x } 300 \\ &= 2250 \text{ mm} \end{aligned}$$

Therefore the total equivalent length of the corner,

$$\begin{aligned} L_T &= R_{CL} + L \\ &= 375 + 2250 \\ &= 2625 \text{ mm} \end{aligned}$$

Finally, the approximate friction loss of the corner, based on the formula for short straight duct is

$$\begin{aligned} K &= 0.01\frac{D+W}{DW} \times L_T \\ &= 0.01\frac{300+300}{300\times 300} \times 2625 \\ &= 0.175 \end{aligned}$$

4.2.2 Straight duct

For short rectangular straight ducts, the losses may be approximated using the following formula;

$$K = 0.01\frac{D+W}{DW} \times L_T$$

4.2.3 Screens

For screens, many of the turbulent reduction theories are based on a pressure loss coefficient, K defined as;

$$K = K_0 + \frac{55.2}{\mathrm{Re}_d}$$

where

$$K_0 = \left(\frac{1-0.95\beta}{0.95\beta}\right)^2$$

$$\beta = \frac{\text{projected open area}}{\text{total area}} = \left(1 - \frac{d}{M}\right)^2$$

d = wire diameter

M = mesh length

Re_d = Reynolds number based on wire diameter, d

Assuming a wire diameter, d = 1 mm and an opening ratio, β = 0.7, K_0 = 0.254. With the operating temperature of 300 °C and velocity of 2.5 m/s, the Reynolds number based on the wire diameter, Re_d is calculated as 51350. This yields a loss factor, K = 0.3.

4.2.4 Honeycombs

Generally, losses in honeycombs with a length/diameter = 6, and equal tube areas are given in Fig 4.2. However, these losses are usually very small (< 5 % of the total tunnel loss), and therefore are usually ignored.

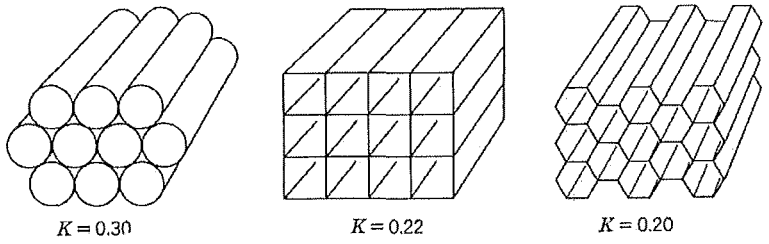

(Adopted from ref [14])

Figure 4.2 Some honeycombs and their losses.

4.2.5 Heating element

The manufacturer should be consulted for the pressure drop across the heating element. However, such information was not available from the supplier of the heating element being used in this application. Thus a typical value of 20 Pa based on local suppliers was used. This value must be revised if better estimation is desired.

4.3 Dampers

Because of the recirculation of air within the closed-loop, and that the air will be heated during operation, internal pressure would build up in the tunnel. Thus a relief damper (Fig. 4.3) was installed downstream of the test section for the purpose of

preventing such pressure build up. The fact that the relief damper was installed downstream of the test section would also minimise leakages into the test section, as only the section downstream of the test section is close to atmospheric pressure.

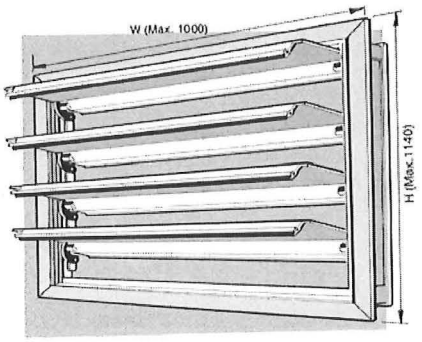

(Adopted from ref [28])

Figure 4.3 Typical layout of a relief damper

A louvre damper (volume control damper) (Fig. 4.4) was installed along the return passage to introduce fresh air into the wind tunnel. It was located close to the fan inlet so that the fan's suction is sufficient to get the fresh air into the tunnel, and also that good mixing of the two air streams (fresh and return air) could be achieved. The level of mixing between the fresh air and the return air could be controlled by adjusting the opening area (blades) of the damper.

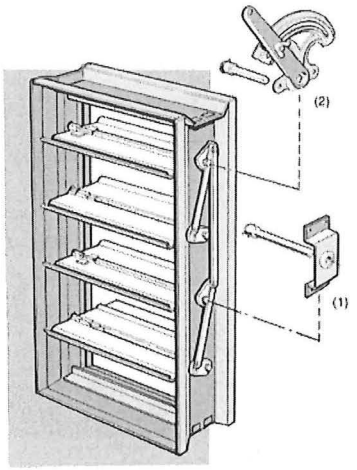

(Adopted from ref [28])

Figure 4.4 Typical layout of a louvre damper (volume control damper)

4.4 Fan and heating elements

With the volumetric flow and system resistance determined, it is now possible to select a fan, which would meet the requirements. Based on the discussions in previous sections, it was decided to use a centrifugal fan instead of an axial fan, mainly for the following reasons;

1. Physical size

   A centrifugal fan is capable of delivering the same quantity of air and pressure as an axial fan, but at a smaller size.

2. Performance

   A centrifugal fan is known to operate more efficiently than an axial fan, at a much lower noise level.

After consulting with several fan suppliers, it was decided to use a single inlet centrifugal fan, with the operating point of 0.225 m^3/s at 100 Pa as the pressure losses within the tunnel are much lower than this pressure. However, it was soon discovered that the fan selected was inappropriate for this type of application, mainly because of the elevated operating temperature of 300 °C of the recirculating air. The temperature rating of a typical fan ranges from ambient to approximately 70 °C. Therefore at such a high temperature, the impeller would soften and jeopardise the fan's performance. Furthermore, the motor itself would not sustain such temperature.

Three suggestions have been proposed to solve the problem. The first, is to lower the operating temperature from 300 °C to whatever temperature is appropriate for the fan to operate. This however, would mean that the ability of the wind tunnel to conduct sprinkler testing was compromised. The second option is to use a high temperature rated fan (made out of stainless steel). The third option was to change the wind tunnel design from a closed-circuit to an open type. This way, the fan would stay clear of the high temperature airflow, and only operate at ambient conditions. It also means that smoke has to be supplied continuously to the wind tunnel during the smoke detector tests since recirculation is no longer available.

After careful consideration, the second option was preferred over the first option, because it enabled both sprinkler and smoke detector tests to be conducted, as initially planned. However, using such a fan would incur an extremely high cost (approximately NZ$ 5,000), on top of the 8 weeks delivery time (including the Christmas and New Year holiday). Due to limited resources, as well as the time that was available for the completion of this research, the second option was deemed infeasible, and thus the third option was considered in more detail.

With the open type design, the typical fan (NZ$ 250) could be used since it only operates under the ambient condition. However, it was anticipated that the power required for the heating elements would increase dramatically, since the airflow has to be heated from ambient to 300 °C in one pass (no recirculation). A rough calculation estimated that a 81 kW heating element would be needed to achieve this. For recirculating air, only 3 kW is needed (refer *Appendix 2* for calculations). Note that the calculations assume that the airflow is flowing pass a cylinder (representation of heating element) and ignore any heat losses through the duct's envelope. As such, it is anticipated that a higher power will be needed to achieve the required temperature. The actual heating power will be justified during the testing and commissioning of the wind tunnel.

Calculation:

Since the volumetric flow rate, $Q_{dot} = 0.225\ m^3/s$, and density of air, $\rho = 1.278\ kg/m^3$ at ambient condition, thus the mass flow rate,

$$\begin{aligned} m_{dot} &= \rho \times Q_{dot} \\ &= 1.278 \times 0.225 \\ &= 0.288\ kg/s. \end{aligned}$$

Therefore, the power required to heat this volume of air from ambient to 300 °C in one pass,

$$\begin{aligned} P &= m_{dot} \times C_p \times \Delta T \\ &= 0.288 \times 1 \times (300 - 20) \\ &= 81\ kW. \end{aligned}$$

With the power of the heating elements determined, several suppliers were consulted for the cost of supplying the 81 kW duct heater (terminal box & heating elements). The quoted price for the duct heater was approximately NZ$ 5,500, which was again too costly for the project.

So the choices were down to two options:

1. To get a typical fan with an expensive heater (81 kW), or
2. To get an expensive fan with an inexpensive heater (3 kW).

However, none of the two options was acceptable because the expensive item in either option has exceeded the budget that was set for this project. Furthermore, the cost of constructing the wind tunnel itself, as well as the cost of other components that are to be installed has not yet been included.

Consequently, an alternative design was proposed as a potential solution to solve the cost issue (i.e. to have a standard fan, and the 3 kW heater) (Fig. 4.3).

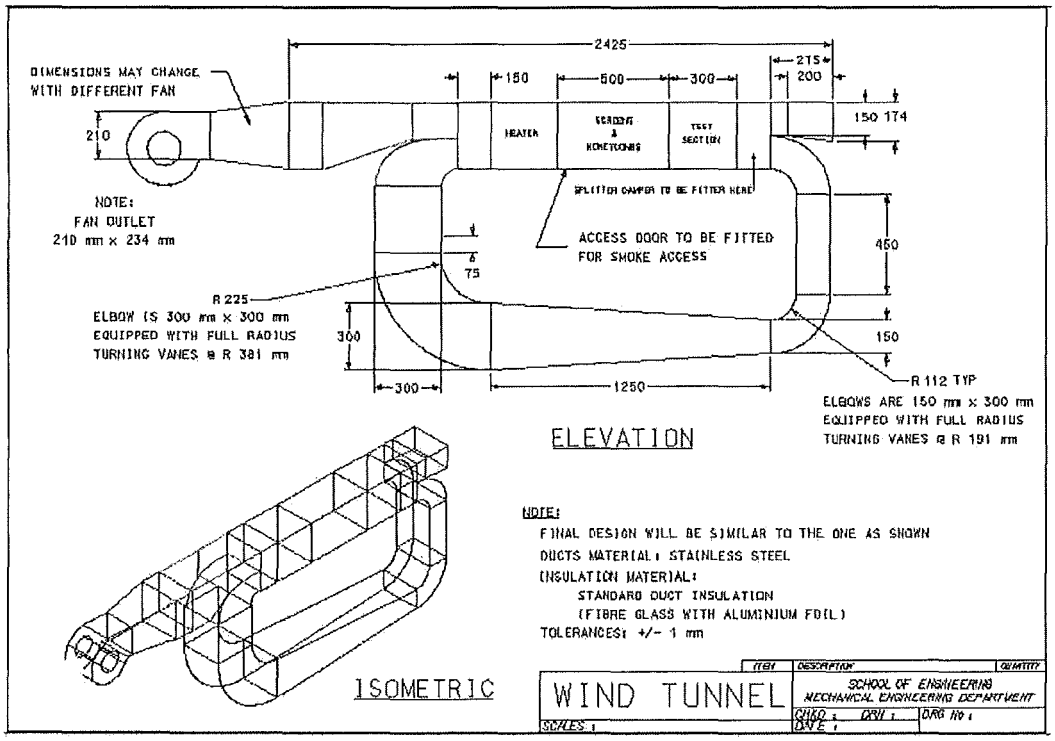

Figure 4.3 Alternative design of wind tunnel

This design consists of a combination of an open type and closed-circuit wind tunnel. It is similar to the initial idea of having the closed-circuit to minimise the heating power required, while extending the fan to one end of the wind tunnel so that it is not exposed to the high temperature recirculating air, and only operates in ambient condition.

Initially, fresh air is being supplied into the wind tunnel. The airflow will pass through the heating elements and a series of screens and honeycombs before entering the test section. Upon leaving the test section, a fraction of the airflow will be directed into the loop as the recirculating air, while the rest will be discharged through the outlet. This is done by using a splitter damper. A diffuser is used in the return passage to slow the airflow and thus reduce the losses. A corner, instead of a "Tee" is used as the re-entry of the recirculating air (Fig. 4.4). The problem with using a "Tee" is that the pressure of the fresh air is much higher than the recirculating air, and thus would prevent the recirculating air from re-entering the main tunnel, while the corner would direct the recirculating air to enter in the direction of the fresh air airflow (venturi effect).

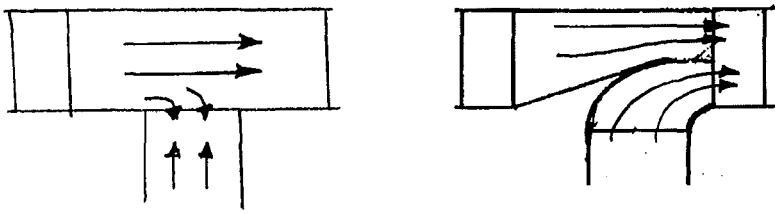

Figure 4.4 Sketch of "Tee" and "corner entry"

While this design seems feasible, and is able to solve the cost issue, a potential problem was soon discovered. Because the fan is continuously supplying fresh air into the wind tunnel, the loop will eventually be pressurized. Consequently, a layer of stagnant air would be expected to form in the loop and the lower section of the main tunnel (Fig. 4.5). This phenomenon would effectively turn the wind tunnel into an open type wind tunnel, where most of the fresh air supplied by the fan would be simply discharged through the outlet. Although a small amount of mixing between the recirculating air and fresh air was anticipated, that would not be able to raise the fresh air's temperature significantly enough before it reached the heating elements.

Effectively, the heating elements would be expected to heat the fresh air from ambient to 300 °C, and thus any saving in the power/cost was eliminated.

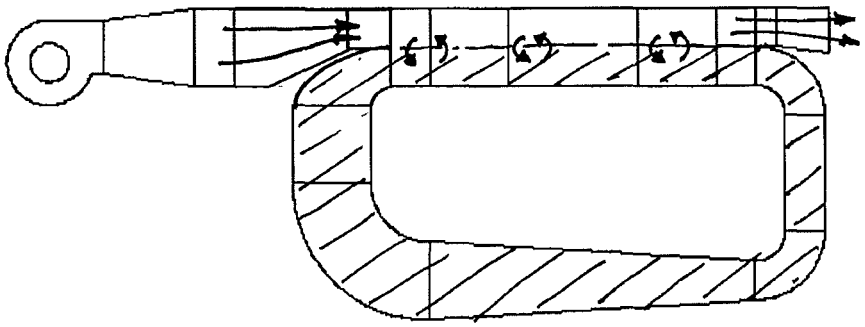

Figure 4.5 A layer of stagnant air formed within the pressurized loop.

Eventually, the original closed-loop design was revisited, but at the expense of the system performance. The final design of the wind tunnel is shown in Fig. 4.6. As indicated by the drawing, the initial design was adopted, with modifications made to the fan. Since the possibility of getting a standard fan off the shelves was not feasible, and importing a high temperature fan proved too costly and long, emphasis were put on customising a fan that would sustain the elevated operating temperature. The idea was to find an impeller and a fan scroll (case) that could sustain the high temperature, while extending the length of the drive shaft so that the motor was located well away from the heat. After thorough searches through some local businesses, such an impeller and scroll (Fig. 4.7) were located from a company, which specializes in gas heating applications. The impeller and scroll were known to be used in the past in space heating applications involving gas burners, thus 300 °C was not considered as an issue.

However, there was a downside to this, because of the age of the fan (> 10 years), little information was available on it, in terms of its performance and capacity. The only information available was that for a 6-inch diameter x 3-inch impeller, the air capacity was about 350 CFM at 1400 RPM (Fig. 4.7). The required volume flow at the test section in terms of CFM is approximately 480 CFM. It was suggested by the supplier that by increasing the size of the impeller to a 7-inch diameter x 3-inch

(which was the biggest size they have in stock anyway), and possibly connecting it to a direct motor drive, which runs at slightly higher RPM, the required volume flow of 480 CFM could be met. Another problem was that no information was provided in terms of the fan's static pressure, thus even if the volumetric flow of 480 CFM could be met, the fan might still not be able to overcome the system resistance.

Despites the unknowns of this proposed solution in terms of performance, this was considered to be the only feasible solution considering the cost of the fan (NZ$ 150 + cost of motor) and the time that was available. The risk involved was considered to be acceptable. Furthermore, the proposed solution would mean that only an inexpensive (3 kW) heating element was needed to raise the air to 300 °C.

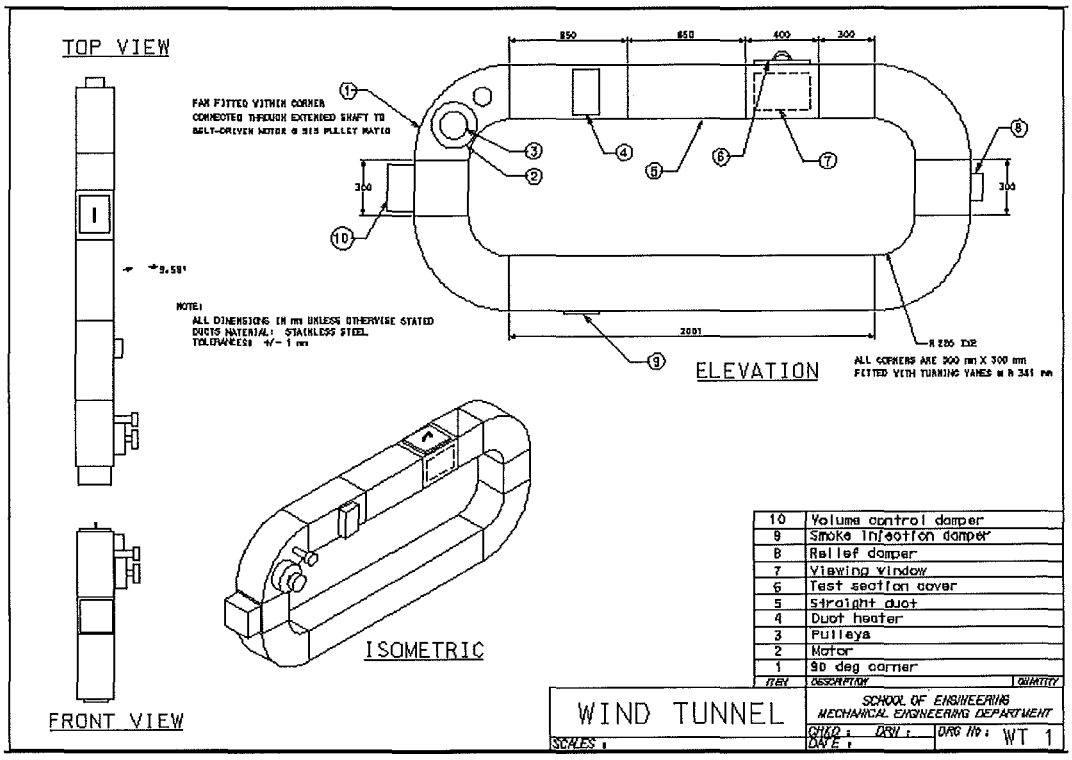

Figure 4.6 The proposed final wind tunnel design.

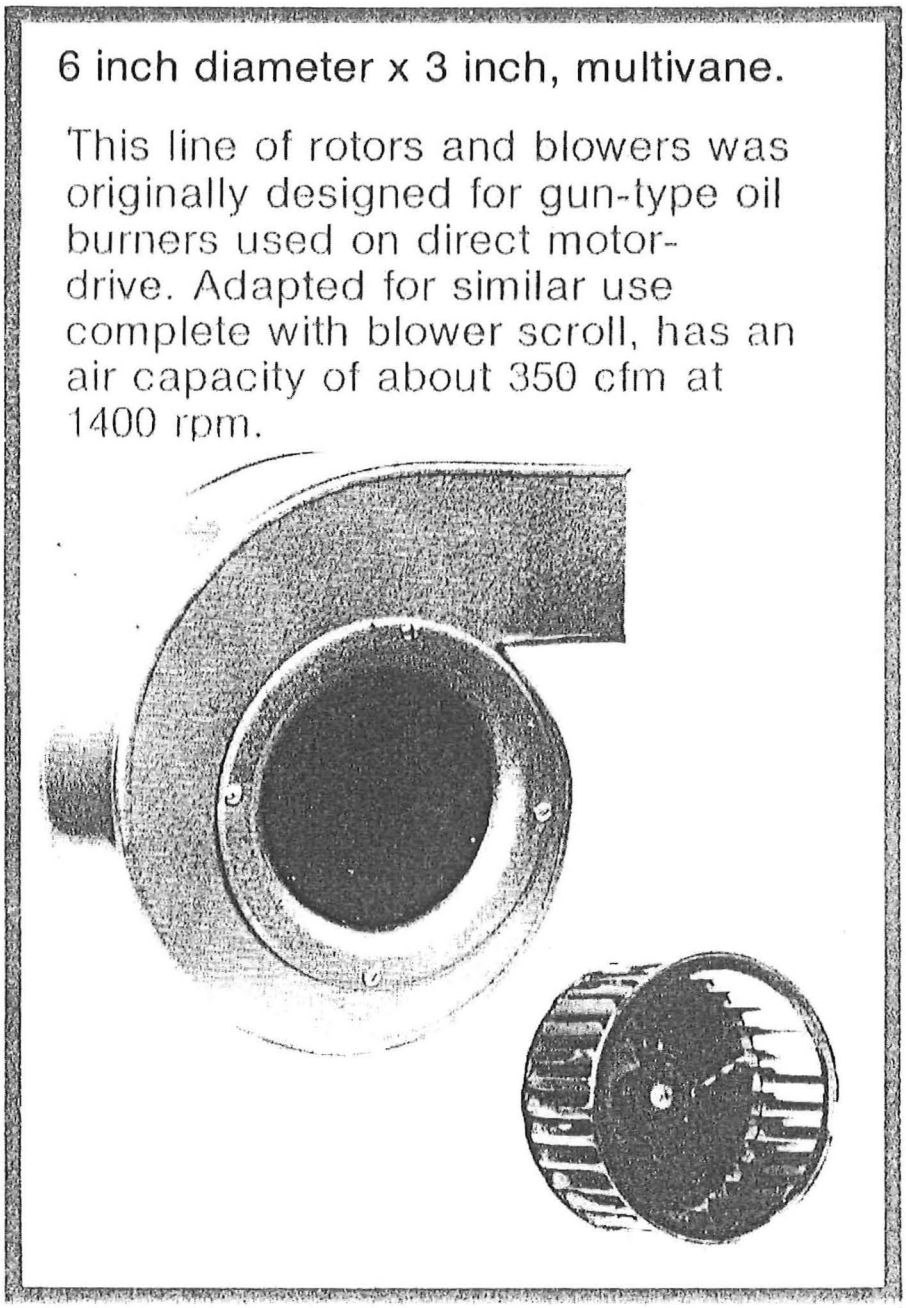

Figure 4.7 The impeller and fan scroll chosen

5. Final design

Fig. 5.1 shows the final design of the wind tunnel. The dampers are yet to be installed.

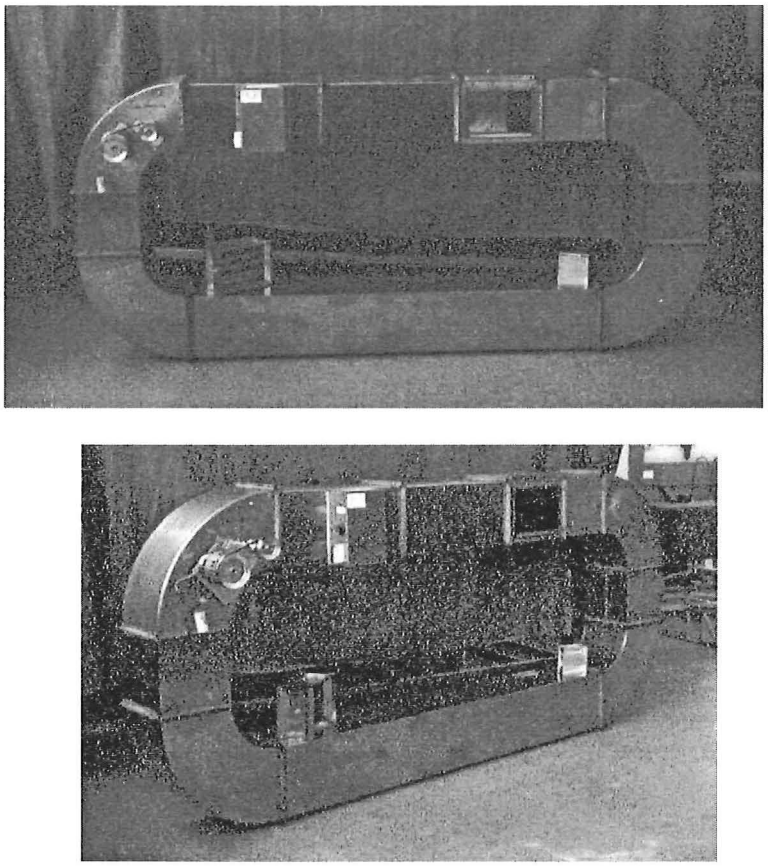

Figure 5.1 Final design of wind tunnel

5.1 Test section

The test section (Fig. 5.2) has a 300 mm x 300 mm square cross-section. It has a viewing window at one side of the wall, and a cover at the top for insertion of test subjects.

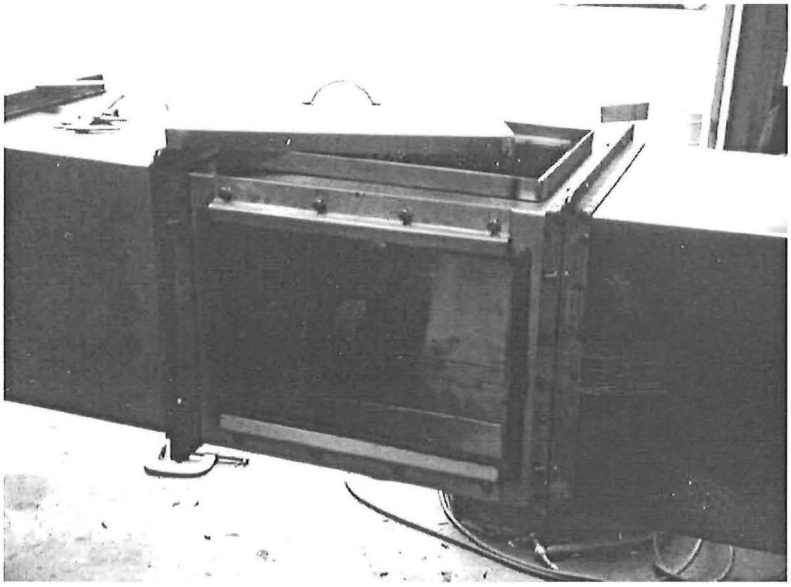

Figure 5.2 Test section

5.2 Screens and honeycombs

The screens and honeycombs are designed with the intention that they could be easily inserted into the tunnel or vice versa during the testing and calibration of the wind tunnel. As such, a box will be constructed to hold the screens in place where they can be inserted or removed from the box with ease (Fig. 5.3).

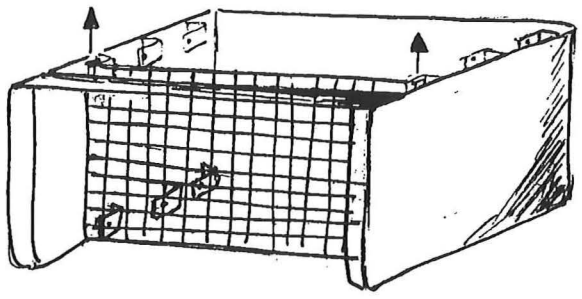

Figure 5.3 Design of the screens and honeycombs "box"

5.3 Corners

The corners were of the single-vaned full radius corner, with the optimum R/D ration of 1.25.

Throat radius = 225 mm

Heel radius = 525 mm

Vane radius = 381 mm

One of the corners was made without turning vane. It was used to conceal the fan within the tunnel in order to create a straight closed-loop impression thus giving a better appearance for the wind tunnel.

5.4 Dampers

The dimension of the relief damper is 150 mm x 150 mm. It was located downstream of the test section to minimise the internal pressure build-up of the recirculating air in the tunnel.

The dimension of the volume control damper is 300 mm x 150 mm. It was located close to the fan's inlet along the return passage to control the mixing of fresh and return air.

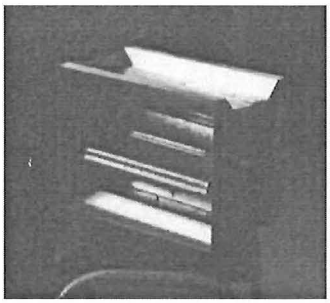

Volume control damper

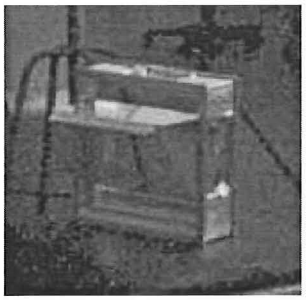

Relief damper

Figure 5.4 The volume control damper and relief damper

5.5 Heating element

The heating element is of 3 kW finned element, equipped with a thermostat, and air pressure switch.

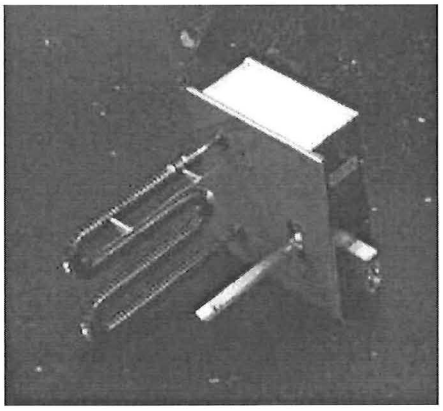

Figure 5.5 The duct heater (heating element plus terminal box)

5.6 *System resistance*

Table 5 shows the estimation of system resistance for the final design.

Table 5 Estimation of system resistance for the final design.

	Section	Dimension (mm)		Length (mm)	k	Velocity (m/s)	Velocity pressure (Pa)		Static pressure (Pa)		Total pressure (Pa)	
		W	D									
1	Sudden expansion (fan's outlet)	Expansion ratio = 2.7			0.70	2.5	1.90	1.90	1.33	1.33	3.23	3.23
2	Straight	300	300	650	0.04	2.5	1.90	3.81	0.08	1.41	1.98	5.21
3	Heater	-	-	-	-	2.5	1.90	5.71	20.00	21.41	21.90	27.12
4	Straight	300	300	650	0.04	2.5	1.90	7.61	0.08	21.48	1.98	29.09
	Screens	-	-	-	1.0	2.5	1.90	9.51	1.94	23.42	3.84	32.94
5	Straight	300	300	400	0.03	2.5	1.90	11.42	0.06	23.48	1.96	34.90
6	Straight	300	300	300	0.02	2.5	1.90	13.32	0.04	23.52	1.94	36.84
7	Elbow (R/D = 1.25)	300	300	2625	0.18	2.5	1.90	15.22	0.33	23.85	2.24	39.07
8	Straight	300	300	300	0.02	2.5	1.90	17.12	0.04	23.89	1.94	41.01
9	Elbow (R/D = 1.25)	300	300	2625	0.18	2.5	1.90	19.03	0.33	24.22	2.24	43.25
10	Straight	300	300	2000	0.13	2.5	1.90	20.93	0.25	24.48	2.16	45.40
11	Elbow (R/D = 1.25)	300	300	2625	0.18	2.5	1.90	22.83	0.33	24.81	2.24	47.64
12	Straight	300	300	300	0.02	2.5	1.90	24.73	0.04	24.85	1.94	49.58
13	Sudden contraction (fan's inlet)	Contraction ratio = 2.2			0.43	2.5	1.90		0.82		2.72	52.30
				TOTAL	**3.0**				**25.67**		**52.30**	

This value has been adjusted to include the effect of density

5.7 Fan

The fan selected consists of a belt-driven 7-inch diameter x 3-inch impeller with scroll, coupled to a 0.3 kW motor with maximum of 1400 RPM. A 5:3 pulley ratio was used to obtain higher fan speed.

The impeller and the scroll were located within the unvaned corner, with the belt drive located at one side of the corner, coupled together using a stainless steel shaft to prevent the heat from being conducted to the motor. One end of the corner was blocked with a piece of sheet metal, except for the fan's outlet to ensure that all the air enters the fan and is only discharged through the outlet (Fig. 5.6)

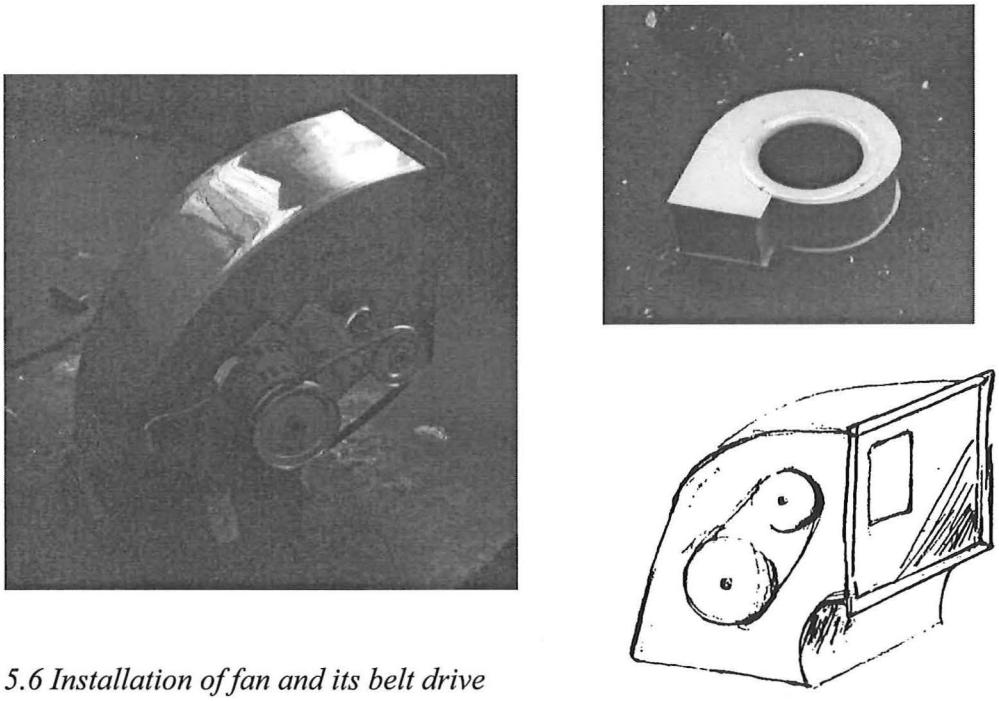

Figure 5.6 Installation of fan and its belt drive

It was anticipated that the sudden expansion at the fan discharge would incur higher pressure losses than if the outlet were connected to an expansion. The same applied to the fan's inlet, where vanes were not provided to guide the airflow into the fan. The reasons that these were done were because of limited time available as well as simplicity. However, if the losses were found to be too great in the future during the testing and calibration, the expansion would be added to the fan's outlet, and a corner added to the fan's inlet (Fig 5.7).

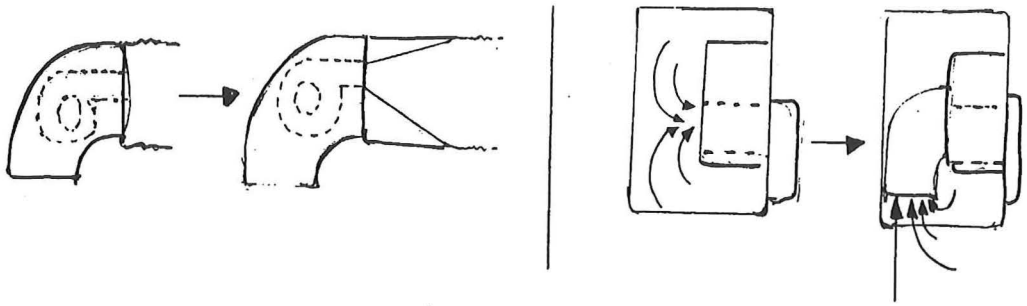

Figure 5.7 Current and recommended fan's inlet and discharge

Unfortunately, neither the fan's characteristic curves nor the operating point of the fan could be determined without performing proper tests and measurements.

5.8 Final fabrication cost

Table 6: Final fabrication cost of wind tunnel

Components	Cost ($)
Sheet metal work (material and labour)	1,200
Duct heater	650
Fan (impeller and scroll)	150
Motor and installation	100
Volume control damper	93
Relief damper	97
Screens & honeycombs	Yet to be costed
Total	**2,290 + GST**

6. Future work

In order to carry out sprinkler and smoke detector tests, the wind tunnel's performance must first be assessed to make sure that the design requirements for the tests are met accordingly. This performance assessment however was not done owing to the lack of time. This chapter outlines the recommendations as how the wind tunnel's performance can be assessed in the future.

Although the wind tunnel consists of a relatively simple ductwork system where the system resistance can be calculated fairly accurately, the fact that little information is available on the fan's performance have made it impossible to check if the fan is suitable for the application. Subsequently, all that can be done is to select what appears to be a suitable fan, fix it to the application and try it. In such an instance it is necessary to measure the volume of air flowing through the fan assembly and the pressure against which the fan is working in order to ensure that the fan assembly delivers the output for which it was designed.

In order to measure the airflow and pressure reliably, it is necessary to understand some of the principles and conditions of air measurement.

6.1 Measurement of air volume

The most usual method of measuring air volume flowing in a duct is to determine by test the average velocity flowing in the section and multiply this velocity by the cross-sectional area of the section. The measurement of average velocity calls for some little care, and what is normally done is to divide the duct cross-section into a number of equal areas, measure the velocity at one or more points within each area, and average the results. Fig. 6.1 shows the methods normally used for rectangular ducts of various sizes.

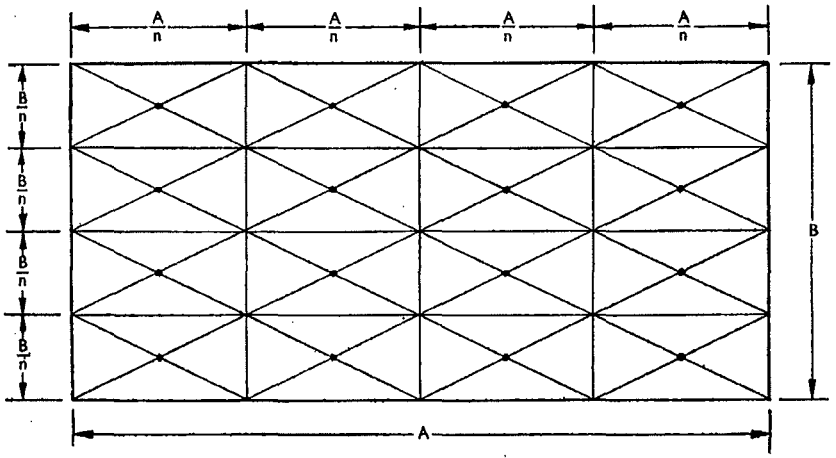

Area of airway in sq. ft.	n
Up to and including 1	3
Over 1 up to and including 4 ...	4
„ 4 „ „ 25 ...	5
„ 25	6

(Adopted from ref [16])

Figure 6.1 Positions of points of measurement in rectangular ducts.

Generally, as the velocity of air in a duct on the intake side of a fan is usually axial and evenly distributed, measurements of airflow should be made there. However, owing to the fan's inlet condition for this application (unguided entry), which could cause turbulence, it is recommended that the velocity measurement to be made at the test section, where the duct is straight and airflow is relatively laminar. Measurements should not be made downstream of any obstructions, enlarging sections, bends etc., owing to risk of air turbulence upsetting continuity of airflow.

6.2 Measurement of pressure

The pressure of the wind tunnel can be measured in terms or static pressure or total pressure. However, it is often done in terms of static pressure. Measuring the static pressure difference is not an easy task. Usually, it should be done in a plain straight duct, with some form of straightening vanes to damp out any rotation and unwanted pulsations in the airflow, as shown in Fig. 6.2. Note that in some instances, heater, filters etc., may make fairly efficient straighteners, although allowance must be made for the pressure drop across them.

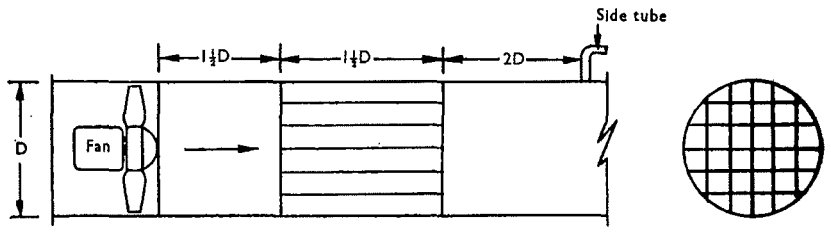

(Adopted from ref [16])

Figure 6.2 Straightening vanes in test ducts and recommended static pressure tapping

As fas as possible, the static pressure tappings should not be made immediately downstream of fans, bends, or obstructions. It is often a good plan to make readings fairly remote from the fan when the resistance to airflow between inlet and pressure tapping is easily calculate, or not very high. Therefore it is recommended that the static pressure tappings be made before and after the test section.

The total pressure at any point in a system should be determined by adding to the static pressure, the velocity head computed from the average velocity flowing in the section of duct considered.

6.3 Methods of measurement

6.3.1 Pitot-static tube

There are many ways of measuring air velocities and pressures. The most common device for determining the air velocities and pressures is the pitot-static tube. A standard pitot-static tube is shown in Fig. 6.3. It comprises a double tube, one inside another, bent a t right angle. The outer tube has a number of holes in its sides as illustrated. The device is inserted into an air duct with its open end facing the direction or airflow. The holes in the side of the outer tube are consequently at right angles to the airflow.

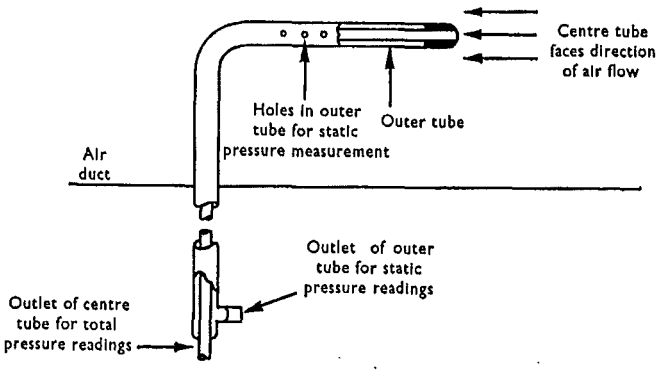

{Adopted from ref [16]}

Figure 6.3 Standard Pitot-static tube.

Total pressure can be measured by a single tube facing the direction of airflow, known as a facing tube. In that case to obtain a velocity reading it is necessary to make a separate measure of static pressure and subtract that from the total pressure. The pitot-static tube permits a direct reading of velocity pressure by connecting the two outlets of the tube to a pressure-indicating device. The inner section of the tube, whose open end faces the airflow, receives the impact of air velocity and communicates total pressure, $\left(p+\frac{1}{2}\rho V^2\right)$. The outer section, whose holes are not affected by velocity, communicates only static pressure, p. Subsequently, the pressure differential indicated by the pressure-indicating device would be the velocity pressure, $\left(\frac{1}{2}\rho V^2\right)$, from which the velocity may be calculated. Note that care must be taken to see that the tube faces directly into the airflow.

6.3.2 The hot wire anemometer

This device is usually used for very sensitive measurements of air velocity, particularly of low velocities. It comprises a fine platinum wire which is inserted in the airflow and heated by an electric current. The temperature of the wire at a given current flow is influenced by the cooling effect of the moving air. A high velocity airflow will have greater cooling effect than a low velocity. The resistance of the wire changes with temperature. Consequently, as its temperature changes with variation in air velocity so does its resistance. Measurement of the resistance of the wire at a given

current flow indicate the velocity. The hot wire anemometer is extremely sensitive to low air velocities but is not sensitive to changes in direction of airflow.

6.3.3 Thermocouples

In order to measure the temperatures of the airflow, a thermocouple tree would be placed in the instrumentation section prior to the test section. It is recommended that the thermocouples be spaced in accordance to Fig. 6.1.

7. Conclusions

Many tests have been conducted by various organizations with regards to sprinklers and smoke detectors, using specifically designed apparatus such as the plunge test apparatus and the FE/DE apparatus. These apparatus, however are only intended for the specified test, and none of them are able to be used for other tests.

The wind tunnel described in this report is designed with the ability to integrate both sprinkler and smoke detector tests into the same apparatus. It consists of a closed-loop, which incorporates features from both the plunge test apparatus and the FE/DE apparatus. The design requirements are airflow velocity up to 2.5 m/s with a maximum temperature of approximately 300 °C at the test section. The test section has a square cross section of 300 mm x 300 mm, with a viewing window fitted to one side of the wall, and an access door fitted at the top for insertion of test subjects. Screens and honeycombs are used to obtain high quality airflow across the test section. Corners are fitted with turning vane to minimise pressure losses. A fresh air damper is fitted prior to the fan intake to supply fresh air into the recirculating airflow, while a relief damper is fitted downstream of the test section to relief the internal pressure built up owing to the recirculation. The fan assembly consists of a 7" diameter x 3" impeller and scroll, connected to a belt-driven 0.3 kW motor. The system resistance of the final design is estimated to be 26 Pa.

The performance of the wind tunnel is not assessed owing to the lack of time. However, it is recommended that the volume flow/airflow velocity measurements to be made in the test section, as illustrated in Fig. 6.1. Any pressure tappings, if necessary should be made before and after the test section, as illustrated in Fig. 6.2. The airflow temperature is to be measured using a thermocouple tree, located at the centreline of the wind tunnel prior to the test section. Thermocouples should be spaced in accordance to Fig. 6.1.

If future improvements are necessary in terms of reducing the system resistance, it is recommended that the fan assembly (fan's inlet and outlet condition) be modified as suggested in section 5.6.

References

1. *UL 217: Standard for Single and Multiple Station Smoke Detectors,* Underwriters Laboratories, Inc., Northbrook IL, 1993.
2. *UL 268: Standard for Smoke Detectors for Fire Protective Signalling Systems,* Underwriters Laboratories, Inc., Northbrook IL, 1993.
3. *UL 268A: Standard for Smoke Detectors for Duct Application,* Underwriters Laboratories, Inc., Northbrook IL, 1993.
4. Factory Mutual Research *Smoke Actuated Detection for Automatic Fire Alarm Signalling, Class Numbers 3230 to 3250.*
5. *EN54: Components of Automatic Fire Detection Systems,* European Committee for Standardization, Parts 1-9, 1998.
6. Grosshandler. J. *Towards the Development of a Universal Fire Emulator-Detector Evaluator.* Fire Safety Journal 29, 113 – 128, 1997.
7. Lee; Thomas G. K. *An Instrument to Evaluate Installed Smoke Detectors,* NBSIR 78-1430, National Bureau of Standards, Washington, DC, February, 1978.
8. Cleary, T.; Chernovsky, A.; Grosshandler, W.; Anderson, M. *The Fire Emulator/Detector-Evaluator* NIST Internal Report, National Institute of Standards and Technology, Gaithersburg, MD, U.S.A., 1999.
9. Fleming, R. P. *Theory of Automatic Sprinkler Performance,* NFPA Handbook of Fire Protection, 6-113 – 6-115.
10. Cleary, T.; Chernovsky, A.; Grosshandler, W.; Anderson, M. *Particulate Entry Lag in Spot-Type Smoke Detectors.* Fire Safety Science Proceedings of the Sixth International Symposium, 779 – 790.
11. Brozovsky, E.; Motevalli, V.; Custer, R. L. P. *A first approximation method of smoke detector placement based on design fire size, critical velocity, and detector aerosol entry lag time.* Fire Technology Fourth Quarter 1995.
12. Cleary, T.; Grosshandler, W.; Chernovsky, A. *Smoke Detector Response To Nuisance Aerosols.* National Institute of Standards and Technology (NIST), Gaithersburg, MD, U.S.A.
13. *UL199, Standard for Automatic Sprinklers for Fire-Protection Service, 8th edition,* Underwriters Laboratories Inc. Northbrook, IL., 1990.

14. Rae, W. H. JR.; Pope, A. *Low-Speed Wind Tunnel Testing, 2nd Edition.* John Wiley & Sons, Inc. 1984.
15. Stevenson, D. C. Dr. *Design & Construction of Small Wind Tunnels, Part 1: A 12" x 12" General Purpose Tunnel.* Department of Mechanical Engineering, Monash University, Australia.
16. Osborne, W. C.; Turner, C. G. *Woods Practical Guide to Fan Engineering.* Woods of Colchester Ltd., 1952.
17. Bukowski, R. W.; Mulholland, G. W. *Smoke Detector Design and Smoke Properties,* NBS Technical Note 973 U.S. Department of Commerce, National Bureau of Standards, Nov. 1978.
18. *Section A-1-4, Appendix A Explanatory Material,* NFPA 72 National Fire Alarm Code 1996; p. 196.
19. Fleming, J. *Photoelectric vs. Ionization Detectors – A Review of the Literature,* Proceedings Fire Suppression and Detection Research Application Symposium, February 25 – 27, 1998, NFPA, Quincy, MA, 1998 p. 18 – 59.
20. Schifiliti, R. P.; Pucci, W. E. *Fire Detection Modelling: State of the Art,* Fire Detection Inst., Bloomfield, CT, p. 57, 1996.
21. Bukowski, R. W.; Averill, J. D. *Methods for Predicting Smoke Detector Activation,* Building and Fire Research Laboratory, National Institute of Standards and Technology, Gaithersburg, MD 20899, USA., 1998.
22. Heskestad, G., *Generalized Characterization of Smoke Entry and Response for Products of Combustion Detectors,* Proceedings of the Fire Detection for Life Safety Symposium, March 31 – April 1, 1975.
23. Bright, R. G. *Recent Advances in Residential Smoke Detectors,* Fire Journal, Volume 69, Number 6 (November 1974), p. 69 – 77.
24. Bukowski, R. W.; Budnick, E. K.; Schemel, C. F. *Estimates of the Operational Reliability of Fire Protection Systems,* International Conference on Fire Research and Engineering, Third Proceedings. October 4-8, 1999, Chicago, IL.
25. Madrzykowski, D. *Evaluation of sprinkler activation prediction methods,* Building and Fire Research Laboratory, National Institute of Standards and Technology, Gaithersburg, MD, USA., 1995.
26. *Handbook of Air Conditioning System Design,* Carrier Air Conditioning Company., 1977.

27. *Understanding Fan Curves,* Twin City Fan Companies Ltd., 2001.

28. *Air Distribution Systems Component Manual,* Holyoake Industries Ltd.

Nomenclature

τ	Time constant
m	mass (kg)
C_p	Specific heat (kJ/kg.K)
h_c	Convective heat transfer coefficient (kW/m.K)
A	Area (m^2)
U	Velocity (m/s)
RTI	Response time index
C	Conductivity factor
L	Characteristic length (m)
Nu_x	Nusselts number
Re_x	Reynolds number
Pr_x	Prantl number
ρ	Air density (kg/m^3)
k	Thermal conductivity (kW/m.K)
K	Pressure loss factor
β	Total area ratio (for screens)
M	Mesh length (m)
ΔP	Pressure difference (Pa)
ΔT	Temperature difference (^oC)
SP	Static pressure (Pa)
BHP	Brake horse-power (kW)
$\dot{Q}$	Volume flow rate (m^3/s)
$\dot{m}$	Mass flow rate (kg/s)

Useful data

VELOCITY

British	*Multiply by*	*Metric*
Feet/minute	0.01667	Feet/second
	0.01136	Miles/hour
Feet/second	1.097	Kilometers/hour
	0.5921	Knots
	0.6818	Miles/hour
Miles/hour	0.447	Meters/second
	1.467	Feet/second
	1.609	Kilometers/hour
	0.8684	Knots
Kilometers/hour	0.9113	Feet/second
	0.5396	Knots
	0.6214	Miles/hour
	0.2778	Meters/second
Meters/second	3.281	Feet/second
	3.6	Kilometers/hour
	2.237	Miles/hour
Knots	1.152	Miles/hour

PRESSURE

British	*Multiply by*	*Metric*
Pounds/square inch	51,710	Microns
	0.06804	Atmospheres
	2.036	Inches of mercury
	703.1	Kilograms/square meter
Pounds/square foot	0.1924	Inches of water
	4.883	Kilograms/square meter
Atmospheres	76.0	Centimetres of mercury
	29.92	Inches of mercury
	1.033	Kilograms/square meters
	14.7	Pounds/square inch
	2116	Pounds/square foot
Inches of water	5.204	Pounds/square meter
	25.40	Kilograms/square meter
	0.07355	Inches of mercury
Kilograms/square meter	0.2048	Pounds/square foot
Microns (of mercury)	0.00001934	Pounds/square inch

WEIGHTS AND MEASURES

British to Metric		*Metric to British*	

LINEAR MEASURE

1 inch	= 25·4 mm.	1 mm.	=	0·03937 inch
1 foot	= 30·4799 cm.	1 cm.	=	0·3937 inch
1 yard	= 0·914399 metre	1 metre	=	39·3701 inch 3·2808 feet 1·09361 yard
1 furlong	= 201·168 metres			
1 mile	= 1·6093 km.	1 km.	=	0·6214 mile

SQUARE MEASURE

1 sq. inch	= 6·4516 sq. cm.	1 sq. cm.	=	0·155 sq. inch
1 sq. foot	= 929·032 sq. cm.	1 sq. metre	=	10·7639 sq. feet 1·1960 sq. yard
1 sq. yard	= 0·8361 sq. m.			
1 acre	= 0·4047 hectare	1 hectare	=	2·4711 acres
1 sq. mile	= 259·00 hectares			

CUBIC MEASURE

1 cu. inch	= 16·387 cu. cm.	1 cu. cm.	=	0·061 cu. inch
1 cu. foot	= 0·028317 cu. m.	1 cu. metre	=	35·3148 cu. feet 1·307954 cu. yard
1 cu. yard	= 0·764553 cu. m.			

LIQUID MEASURE

1 pint	= 0·568 litre	1 litre	=	1·7598 pint
1 quart	= 1·136 litre			
1 gallon	= 4·546 litres			

WEIGHT

Avoidupois		*Avoidupois*	
1 grain	= 0·0648 gramme	1 milligram	= 0·015 grain
1 dram	= 1·772 gramme	1 gramme	= 15·432 grains
1 oz.	= 28·35 grammes	1 kilog.	= 2·2046 lb.
1 lb.	= 0·4536 kilog.	1 quintal	= 1·968 cwt.
1 cwt.	= 50·80 kilog.	1 tonne	= 0·9842 ton
1 ton	= 1016 kilog. 1·016 tonne		

Troy		*Troy*	
1 grain	= 0·0648 gramme	1 gramme	= 0·03215 oz. 15·432 grains
1 dwt.	= 1·5552 grammes		
1 oz.	= 31·1035 grammes		

Adopted from ref [16]

Appendices

Appendix 1 Summary of Fan Laws

Adopted from ref [26]

VARIABLE	CONSTANT	NO.	LAW	FORMULA
SPEED	Air Density Fan Size Distribution System	1	Capacity varies as the Speed.	$\frac{Q_1}{Q_2} = \frac{N_1}{N_2}$
		2	Pressure varies as the square of the Speed.	$\frac{P_1}{P_2} = \left(\frac{N_1}{N_2}\right)^2$
		3	Horsepower varies as the cube of the Speed.	$\frac{Hp_1}{Hp_2} = \left(\frac{N_1}{N_2}\right)^3$
FAN SIZE	Air Density Tip Speed	4	Capacity and Horsepower vary as the square of the Fan Size.	$\frac{Q_1}{Q_2} = \frac{Hp_1}{Hp_2} = \left(\frac{D_1}{D_2}\right)^2$
		5	Speed varies inversely as the Fan Size.	$\frac{N_1}{N_2} = \frac{D_1}{D_2}$
		6	Pressure remains constant.	$P_1 = P_2$
	Air Density Speed	7	Capacity varies as the cube of the Size.	$\frac{Q_1}{Q_2} = \left(\frac{D_1}{D_2}\right)^3$
		8	Pressure varies as the square of the Size.	$\frac{P_1}{P_2} = \left(\frac{D_1}{D_2}\right)^2$
		9	Horsepower varies as the fifth power of the Size.	$\frac{Hp_1}{Hp_2} = \left(\frac{D_1}{D_2}\right)^5$
AIR DENSITY	Pressure Fan Size Distribution System	10	Speed, Capacity and Horsepower vary inversely as the square root of Density.	$\frac{N_1}{N_2} = \frac{Q_1}{Q_2} = \frac{Hp_1}{Hp_2} = \left(\frac{W_2}{W_1}\right)^{1/2}$
	Capacity Fan Size Distribution System	11	Pressure and Horsepower vary as the Density.	$\frac{P_1}{P_2} = \frac{Hp_1}{Hp_2} = \frac{W_1}{W_2}$
		12	Speed remains constant.	$N_1 = N_2$

Appendix 2 Estimation of the heating power required for a closed-circuit tunnel with recirculating air

The heating power required to raise the airflow temperature from ambient to 300 °C in one pass is calculated as followed:

For heat conduction of a cylinder with internal heating (heating element);

Assuming 1-D heat conduction with constant thermal conductivity, the temperature distribution of the cylinder is defined as

$$T(r) = \frac{\dot{q} r_o}{4k}\left(1 - \frac{r^2}{r_o^2}\right) + T_s$$

To relate the surface temperature of the cylinder to the temperature of the incoming fluid, the surface energy is balanced.

$$\dot{q}(\pi r_o^2 L) = h(2\pi r_o L)(T_s - T_a)$$

Rearranging the terms yield

$$T_s = T_a + \frac{\dot{q} r_o}{2h}$$

But the convective heat transfer coefficient, $h = Nu\left(\frac{k}{D}\right)$ and for forced convection

$$Nu = C\,\mathrm{Re}^n\,\mathrm{Pr}^{1/3}$$

Note:

All terms are evaluated at T_a.

Calculation:

The air properties at T_a = 300 °C are;

Density, ρ = 0.6088 kg/m3

Dynamic viscosity, μ = 2.904 x 10^{-5} kg/ms

Pr = 0.684

Assuming the diameter of the cylinder, D = 0.05 m;

$$\text{Re} = \frac{\rho VD}{\mu}$$
$$= \frac{0.6088 \times 2.5 \times 0.05}{2.964 \times 10^{-5}}$$
$$= 2567$$

From table , C = 0.683, n = 0.466

Therefore the Nusselts number;

$$Nu = 0.683 \times 2567^{0.466} \times 0.684^{1/3}$$
$$= 23.35$$

Hence, the convective heat transfer coefficient,

$$h = 23.35 \times \frac{0.0453}{0.05}$$
$$= 21.15 \ {}^{W}/_{m^2 K}$$

Subsequently, raising the airflow temperature to 300 °C using a 3 kW heating element will require an element's surface temperature of

$$T_s = 300 + \frac{3 \times 10^3 \times 0.05}{2 \times 21.15}$$
$$= 303.5^{o} C$$

Since the maximum element's surface temperature (given by the supplier) is 400 °C, therefore the mean of achieving the airflow temperature of 300 °C using a 3 kW heating element is justified.

Appendix 3 Chart for determining vanes location for corners

Adopted from ref [26]

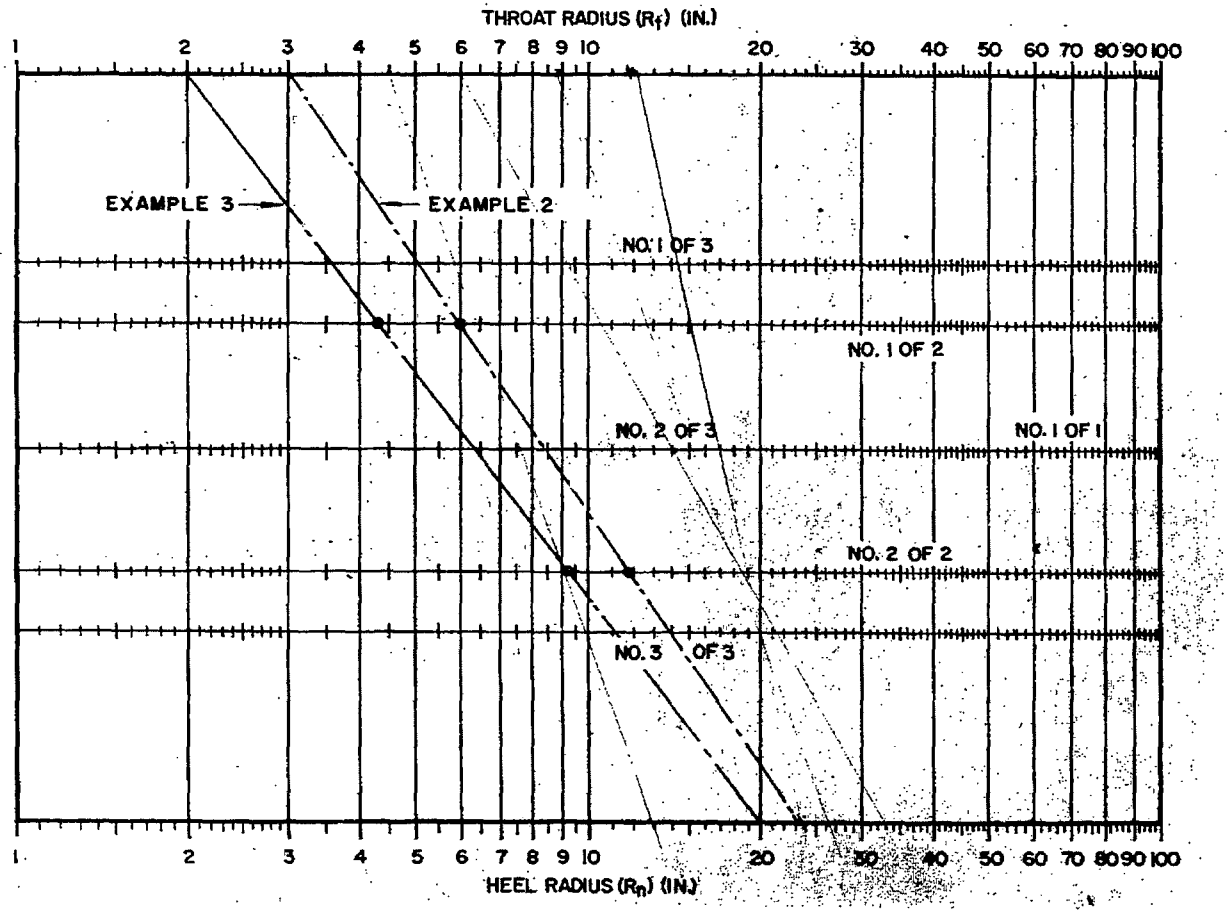

Appendix 4 Spreadsheet for estimating system resistance

Operating parameters

Temperature, T =	300	°C
	573	K
Velocity, V =	2.5	m/s
Air density at T, ρ (T) =	0.6088	kg/m^3
μ (T) =	0.00002964	kg/ms

{ Evaluated at operating temperature }

90° Elbow

Enter the depth, D =	300	mm
	11.8	in.

(1mm = 0.03937 inch)

Enter the throat radius, Rt =	225	mm
	11.8	in.

Therefore,

Heel radius, Rh =	525	mm
	23.6	in.

From Chart 6 of Handbook of Air-conditioning design,

Radius of vane 1, R1 =	381	mm
	15.0	in.
Radius of vane 2, R2 =		mm
		in.

Since R = Rt + D/2

R =	375	mm
	17.7	in.

(Radius of the elbow centre-line)

Thus,

R/D = 1.25

From ref [26] Table 10, with R/D = 1.25 for a rectangular vaned radius elbow with a single vane,

L/D =	7.5	
Equivalent length, L =	2625	mm
	88.6	in.

Resistance k = **0.175**

Straight section

Enter the width, w =	300	mm
Enter the depth, D =	300	mm
Area, A =	0.09	m^2
Enter the length, L =	300	mm
Resistance k =	**0.02**	

Screens

Settling chamber diameter, D =	330	mm		(Equivalent diameter of 300 mm^2 duct)
Enter the diameter of the mesh, d =	1	mm		
The recommended spacing is, s =	660	mm	OR	(2 times the settling chamber diameter)
	30	mm		(30 times the mesh size)
The spacing chosen is =	**30**	mm		

$$\beta = \frac{Projectedopenarea}{Totalarea} = \left(1 - \frac{d}{M}\right)^2$$

d = wire diameter

M = mesh length

Enter the opening ratio, β =	0.7
ko =	0.254
Reynolds number, Re (d) =	51350

$$\mathrm{Re}(d) = \frac{\rho u d}{\mu}$$

$$k_o = \left(\frac{1 - 0.95\beta}{0.95\beta}\right)^2$$

Resistance, k =	0.3
Enter the number of screens, n =	4
Total resistance, k_T =	**1.0**

$$k = k_o + \frac{55.2}{\mathrm{Re}}$$

Honeycomb

Enter the size of the honeycomb, d =	5	mm	
Recommended length =	30	mm	to
	40	mm	

Note:
1) pressure loss across honeycomb is generally small, thus is ignored.

Expansion & Contraction

Enter the duct width, w =	300	mm
Enter the duct depth, D =	300	mm
Area, A =	0.09	m^2
Equivalent diameter, Deq =	0.34	m
Enter the fan's outlet width, w =	100	mm
Enter the fan's outlet depth, D =	125	mm
Area, A =	0.01	m^2
Equivalent diameter, Deq =	0.13	m

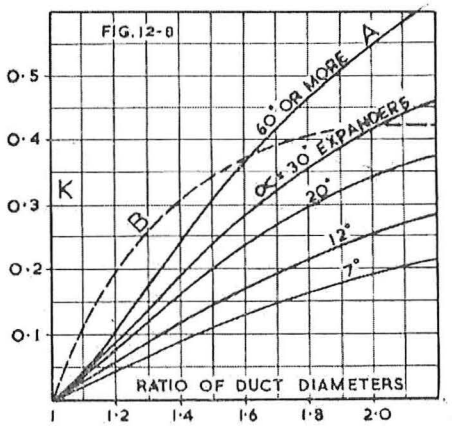

Adopted from ref [16]

(For a sudden expansion, use Curve A)

Ratio of duct diameter, R =	2.7
Resistance, k =	**0.7**

(For a sudden contraction, use Curve B)

Ratio of duct diameter, R =	2.2
Resistance, k =	**0.43**

Appendix 5

Drawing for the Alternative Design and Final Design of Wind Tunnel

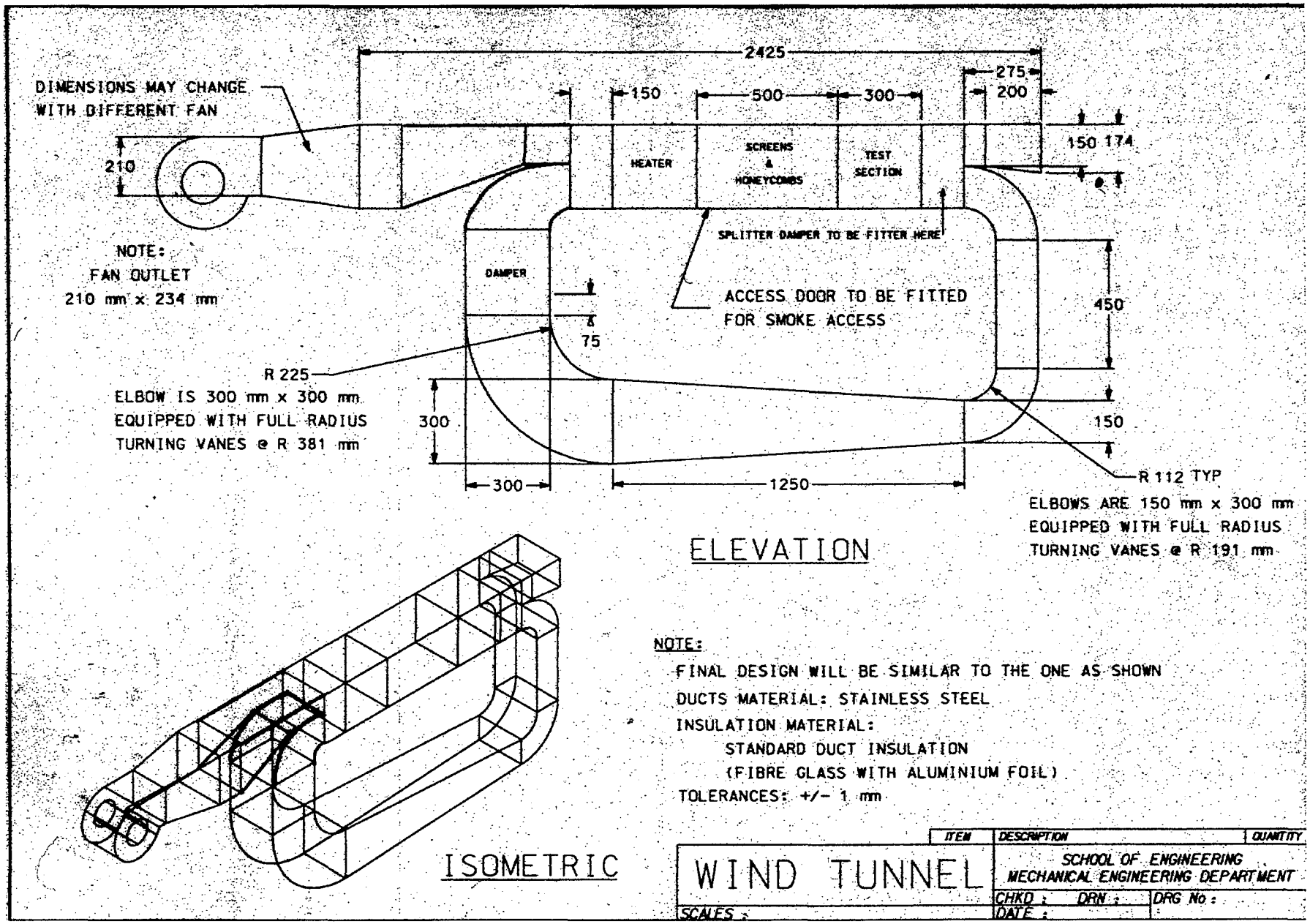
DIMENSIONS MAY CHANGE WITH DIFFERENT FAN
2425
275
200
150
500
300
150 174
210
HEATER
SCREENS & HONEYCOMBS
TEST SECTION
SPLITTER DAMPER TO BE FITTER HERE
NOTE:
FAN OUTLET
210 mm x 234 mm
DAMPER
ACCESS DOOR TO BE FITTED FOR SMOKE ACCESS
450
75
R 225
ELBOW IS 300 mm x 300 mm
EQUIPPED WITH FULL RADIUS
TURNING VANES @ R 381 mm
300
150
300
1250
R 112 TYP
ELBOWS ARE 150 mm x 300 mm
EQUIPPED WITH FULL RADIUS
TURNING VANES @ R 191 mm
ELEVATION
ISOMETRIC
NOTE:
FINAL DESIGN WILL BE SIMILAR TO THE ONE AS SHOWN
DUCTS MATERIAL: STAINLESS STEEL
INSULATION MATERIAL:
STANDARD DUCT INSULATION
(FIBRE GLASS WITH ALUMINIUM FOIL)
TOLERANCES: +/- 1 mm
ITEM
DESCRIPTION
QUANTITY
WIND TUNNEL
SCHOOL OF ENGINEERING
MECHANICAL ENGINEERING DEPARTMENT
CHKD :
DRN :
DRG No :
SCALES :
DATE :

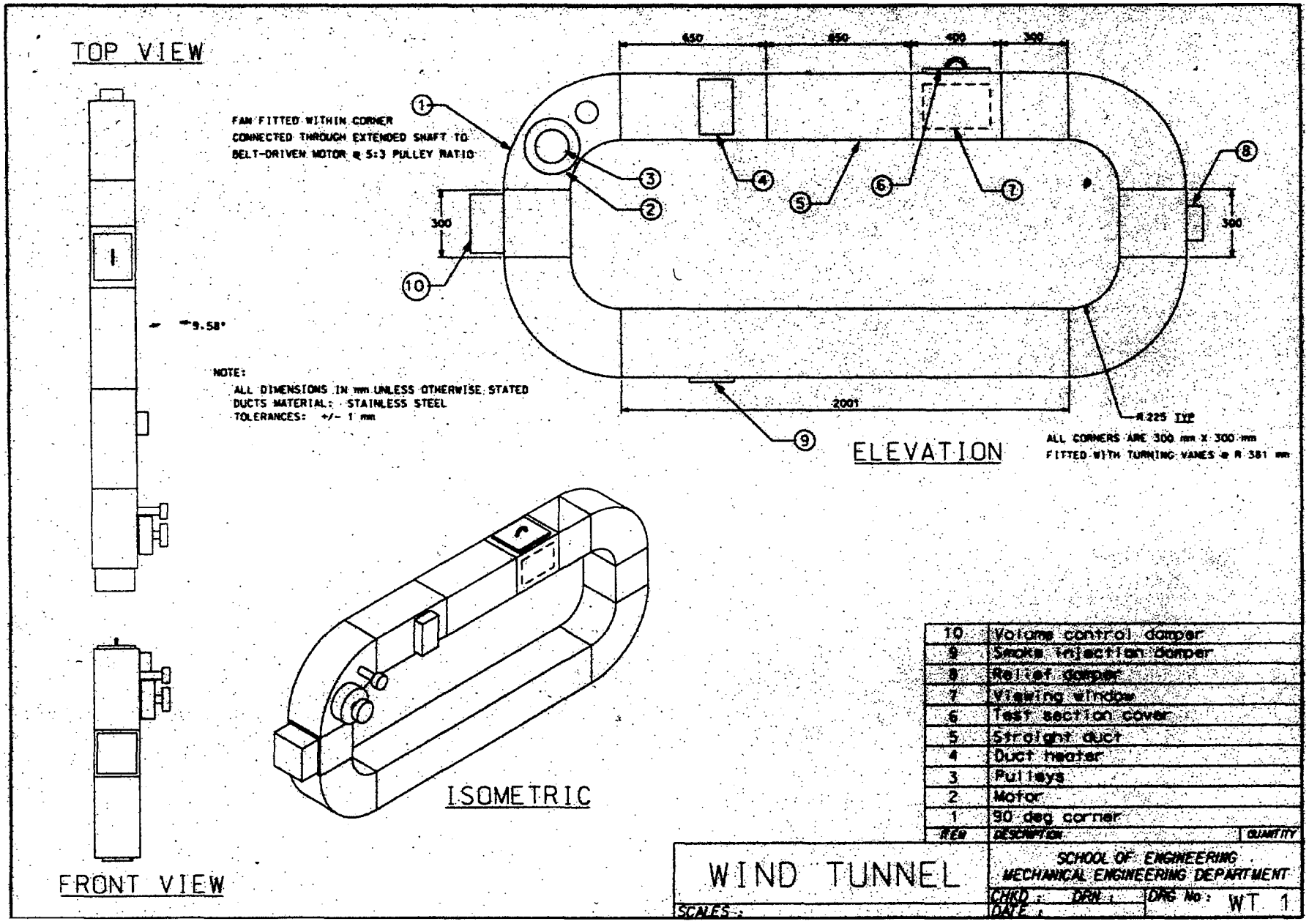
TOP VIEW
FAN FITTED WITHIN CORNER
CONNECTED THROUGH EXTENDED SHAFT TO
BELT-DRIVEN MOTOR @ 5:3 PULLEY RATIO
650
850
400
350
300
300
2001
R 225 TYP
9.58"
NOTE:
ALL DIMENSIONS IN mm UNLESS OTHERWISE STATED
DUCTS MATERIAL: STAINLESS STEEL
TOLERANCES: +/- 1 mm
ELEVATION
ALL CORNERS ARE 300 mm X 300 mm
FITTED WITH TURNING VANES @ R 381 mm
ISOMETRIC
FRONT VIEW
10 Volume control damper
9 Smoke injection damper
8 Relief damper
7 Viewing window
6 Test section cover
5 Straight duct
4 Duct heater
3 Pulleys
2 Motor
1 90 deg corner
REF DESCRIPTION QUANTITY
WIND TUNNEL
SCHOOL OF ENGINEERING
MECHANICAL ENGINEERING DEPARTMENT
CHKD : DRN :
DWG No : WT 1
SCALES :
DATE :

Appendix 6 List of contacts

Fan suppliers

1. *Ivan (Supply of fan's impeller and scroll)*

   Harris Flame Technology.

   41 Braddon Street, Addington, Christchurch.

   Tel: (03) 366 1796

2. *John Gilmour*

   Fantech (NZ) Ltd.

   22 Buchan St. PO Box 25083, Christchurch

   Tel: (03) 379 8622

Heating element suppliers

1. *Cherry (Supply of duct heater)*

   Airflow Engineering (SI) Ltd.

   30c Carlyle Street, PO Box 27-130, Christchurch

   Tel: (03) 365 6278

2. *Colin*

   Avon Electric Ltd.

   Tel: (03) 381 5595

Dampers supplier

1. *Bird*

   Holyoake Industries Ltd.

   27 Wallace Tce, Addington, Christchurch

   Tel: (03) 366 6545

Wind tunnel fabrication

1. *Alastair Young*

   SpiroLoc Tubing,

   41 Barton Street, Woolston, Christchurch

   Tel: (03) 348 2184

FIRE ENGINEERING RESEARCH REPORTS

95/1	Full Residential Scale Backdraft	I B Bolliger
95/2	A Study of Full Scale Room Fire Experiments	P A Enright
95/3	Design of Load-bearing Light Steel Frame Walls for Fire Resistance	J T Gerlich
95/4	Full Scale Limited Ventilation Fire Experiments	D J Millar
95/5	An Analysis of Domestic Sprinkler Systems for Use in New Zealand	F Rahmanian
96/1	The Influence of Non-Uniform Electric Fields on Combustion Processes	M A Belsham
96/2	Mixing in Fire Induced Doorway Flows	J M Clements
96/3	Fire Design of Single Storey Industrial Buildings	B W Cosgrove
96/4	Modelling Smoke Flow Using Computational Fluid Dynamics	T N Kardos
96/5	Under-Ventilated Compartment Fires - A Precursor to Smoke Explosions	A R Parkes
96/6	An Investigation of the Effects of Sprinklers on Compartment Fires	M W Radford
97/1	Sprinkler Trade Off Clauses in the Approved Documents	G J Barnes
97/2	Risk Ranking of Buildings for Life Safety	J W Boyes
97/3	Improving the Waking Effectiveness of Fire Alarms in Residential Areas	T Grace
97/4	Study of Evacuation Movement through Different Building Components	P Holmberg
97/5	Domestic Fire Hazard in New Zealand	KDJ Irwin
97/6	An Appraisal of Existing Room-Corner Fire Models	D C Robertson
97/7	Fire Resistance of Light Timber Framed Walls and Floors	G C Thomas
97/8	Uncertainty Analysis of Zone Fire Models	A M Walker
97/9	New Zealand Building Regulations Five Years Later	T M Pastore
98/1	The Impact of Post-Earthquake Fire on the Built Urban Environment	R Botting
98/2	Full Scale Testing of Fire Suppression Agents on Unshielded Fires	M J Dunn
98/3	Full Scale Testing of Fire Suppression Agents on Shielded Fires	N Gravestock
98/4	Predicting Ignition Time Under Transient Heat Flux Using Results from Constant Flux Experiments	A Henderson
98/5	Comparison Studies of Zone and CFD Fire Simulations	A Lovatt
98/6	Bench Scale Testing of Light Timber Frame Walls	P Olsson
98/7	Exploratory Salt Water Experiments of Balcony Spill Plume Using Laser Induced Fluorescence Technique	E Y Yii
99/1	Fire Safety and Security in Schools	R A Carter

99/2	A Review of the Building Separation Requirements of the New Zealand Building Code Acceptable Solutions	J M Clarke
99/3	Effect of Safety Factors in Timed Human Egress Simulations	K M Crawford
99/4	Fire Response of HVAC Systems in Multistorey Buildings: An Examination of the NZBC Acceptable Solutions	M Dixon
99/5	The Effectiveness of the Domestic Smoke Alarm Signal	C Duncan
99/6	Post-flashover Design Fires	R Feasey
99/7	An Analysis of Furniture Heat Release Rates by the Nordtest	J Firestone
99/8	Design for Escape from Fire	I J Garrett
99/9	Class A Foam Water Sprinkler Systems	D B Hipkins
99/10	Review of the New Zealand Standard for Concrete Structures (NZS 3101) for High Strength and Lightweight Concrete Exposed to Fire	M J Inwood
99/12	An Analytical Model for Vertical Flame Spread on Solids: An Initial Investigation	G A North
99/13	Should Bedroom Doors be Open or Closed While People are Sleeping? - A Probabilistic Risk Assessment	D L Palmer
99/14	Peoples Awareness of Fire	S J Rusbridge
99/15	Smoke Explosions	B J Sutherland
99/16	Reliability of Structural Fire Design	JKS Wong
99/17	Heat Release from New Zealand Upholstered Furniture	T Enright
00/1	Fire Spread on Exterior Walls	FNP Bong
00/2	Fire Resistance of Lightweight Framed Construction	PCR Collier
00/3	Fire Fighting Water: A Review of Fire Fighting Water Requirements (A New Zealand Perspective)	S Davis
00/4	The Combustion Behaviour of Upholstered Furniture Materials in New Zealand	H Denize
00/5	Full-Scale Compartment Fire Experiments on Upholstered Furniture	N Girgis
00/6	Fire Rated Seismic Joints	M James
00/7	Fire Design of Steel Members	K R Lewis
00/8	Stability of Precast Concrete Tilt Panels in Fire	L Lim
00/9	Heat Transfer Program for the Design of Structures Exposed to Fire	J Mason
00/10	An Analysis of Pre-Flashover Fire Experiments with Field Modelling Comparisons	C Nielsen
00/11	Fire Engineering Design Problems at Building Consent Stage	P Teo
00/12	A Comparison of Data Reduction Techniques for Zone Model Validation	S Weaver
00/13	Effect of Surface Area and Thickness on Fire Loads	H W Yii
00/14	Home Fire Safety Strategies	P Byrne
00/15	Accounting for Sprinkler Effectiveness in Performance Based Design of Steel Buildings in Fire	M Feeney

00/16	A Guideline for the Fire Design of Shopping Centres	J M McMillan
01/1	Flammability of Upholstered Furniture Using the Cone Calorimeter	A Coles
01/2	Radiant Ignition of New Zealand Upholstered Furniture Composites	F Chen
01/3	Statistical Analysis of Hospitality Industry Fire Experience	T Y A Chen
01/4	Performance of Gypsum Plasterboard Assemblies Exposed to Real Building Fires	B H Jones
01/5	Ignition Properties of New Zealand Timber	C K Ngu
01/6	Effect of Support Conditions on Steel Beams Exposed of Fire	J Seputro
01/7	Validation of an Evacuation Model Currently Under Development	A Teo
01/8	2-D Analysis of Composite Steel - Concrete Beams in Fire	R Welsh
01/9	Contribution of Upholstered Furniture to Residential Fire Fatalities in New Zealand	C R Wong
01/10	The Fire Safety Design of Apartment Buildings	S Wu
01/11	Smoke Alarm Ownership in Relation to Socio-Economic Factors in Christchurch	N Buchanan
01/12	Accounting for Sprinkler Effectiveness in Performance Based Design of Steel Buildings for Fire	M Feeney
01/13	Equivalent Fire Resistance Ratings of Construction Elements Exposed to Realistic Fires	J Nyman
02/1	Performance of Expanded Polystyrene Insulated Panel Exposed to Radiant Heat	G Baker
02/2	A Comparison Between Predicted and Actual Behaviour of Domestic Smoke Detectors in a Realistic House Fire	D Brammer
02/3	Development of Bench-Scale Testing of Sprinkler and Smoke Detector Activation/Response Time	K S Chin
02/4	The Effect of Door Angle on Fire Induced Flow Through a Doorway	L R Clark
02/5	Implementation of a Glass Fracture Module for the BRANZ Fire Compartment Fire Zone Modelling Software	R Parry
02/6	Assessing the Feasibility of Reducing the Grid Resolution in FDS Field Modelling	N Patterson
02/7	Fire Safety Design of Ferrymead Heritage Park	M Rangi
02/8	Experimental Results for Pre-Flashover Fire Experiments in Two Adjacent ISO Compartments	L Rutherford
02/9	Measurement of Magnitude and Direction of Hot Gas Flow in a Fire Compartment with a Fire-hole Probe	J Schulz
02/10	Assessment of the Current False Alarm Situation from Fire Detection Systems in New Zealand and the Development of an Expert System for Their Identifications	Y F Tu
02/11	Performance of Unprotected Steel and Composite Steel Frames Exposed to Fire	C Wastney

School of Engineering
University of Canterbury
Private Bag 4800, Christchurch, New Zealand

Phone 643 364-2250
Fax 643 364-2758